N-terminal domains mediate [2Fe-2S] cluster transfer from glutaredoxin-3 to anamorsin

This is a post-peer-review, pre-copyedited version of an article published in Nat Chem Biol. 2015 Oct;11(10):772-8. doi: 10.1038/nchembio.1892. Epub 2015 Aug 24. The final authenticated version is available on line at: https://www.nature.com/articles/nchembio.1892

N-terminal domains mediate [2Fe-2S] cluster transfer from glutaredoxin-3 to anamorsin

Lucia Banci[1,2,*], Simone Ciofi-Baffoni[1,2,*], Karolina Gajda[1], Riccardo Muzzioli[1,2], Riccardo Peruzzini[1], Julia Winkelmann[1]

[1]Magnetic Resonance Center CERM, University of Florence, Via Luigi Sacconi 6, 50019, Sesto Fiorentino, Florence, Italy

[2]Department of Chemistry, University of Florence, Via della Lastruccia 3, 50019 Sesto Fiorentino, Florence, Italy

Corresponding authors[*]:

Lucia Banci, E-mail: banci@cerm.unifi.it, Phone: +39-055-4574273, Fax: +39-055-4574923

Simone Ciofi-Baffoni, E-mail: ciofi@cerm.unifi.it, Phone: +39-055-4574192; Fax: +39-055-4574923

Abstract

In eukaryotes, cytosolic monothiol glutaredoxins are proteins implicated in intracellular iron trafficking and sensing via their bound [2Fe-2S] cluster(s). We define here a new role of the human cytosolic monothiol glutaredoxin-3, GRX3, in transferring its [2Fe-2S] clusters to human anamorsin, a physical and functional protein partner of GRX3 in the cytosol, whose [2Fe-2S] cluster-bound form is involved in the biogenesis of cytosolic and nuclear iron-sulfur proteins. Specific protein recognition between the N-terminal domains of the two proteins is the mandatory requisite to promote the [2Fe-2S] cluster transfer from GRX3 to anamorsin.

In eukaryotes, both cytosolic and mitochondrial monothiol glutaredoxin proteins bind [2Fe-2S] clusters in the same way, i.e. via the formation of a [2Fe-2S]-bridged homodimer.[1,2] However, while the molecular function of mitochondrial monothiol glutaredoxins in assisting iron-sulfur (Fe/S) protein maturation by acting as [2Fe-2S] cluster donors towards partner apo proteins has been demonstrated in the last few years,[1,3-6] the question whether cytosolic monothiol glutaredoxins can perform the same function in the cytosol still remains unsolved. On the other hand, the [2Fe-2S] cluster-bound form of cytosolic monothiol glutaredoxins have been recently proposed to be implicated, together with other protein candidates,[7] in cytosolic iron trafficking, playing a crucial role in iron delivery from the cytosolic labile iron pool to virtually all iron-binding proteins in the cell.[8,9] Recently, it has been also shown that, in *Saccharomyces cerevisiae*, the cytosolic monothiol glutaredoxin-3, only when it is complexed with the BolA-like protein Fra2 forming a $[2Fe\text{-}2S]^{2+}$-bridged heterodimer complex, can transfer the cluster to the iron-responsive transcription factor Aft2,[10] in such a way to deactivate the iron regulon for iron uptake.[11-14] Monothiol cytosolic glutaredoxins in cooperation with BolA-like proteins therefore play a key role in regulating iron homeostasis in *Saccharomyces cerevisiae*. However, this function is not conserved in humans as cellular iron homeostasis is regulated at the RNA-level by the iron regulatory proteins 1 and 2.[15] Yeast glutaredoxin-3 alone also can bind a $[2Fe\text{-}2S]^{2+}$-cluster in a homodimeric form with the cluster coordinated by the cysteine residue of the conserved CGFS motif of each monomer and by two glutathione (GSH) molecules.[16] However, unlike the heterodimeric species between glutaredoxin-3 and Fra2, the $[2Fe\text{-}2S]^{2+}$ cluster-bound form of yeast glutaredoxin-3 is unable to transfer the cluster to Aft2. [10] Thus, despite what it has been observed for mitochondrial monothiol glutaredoxins,[1] evidences showing that the homodimeric [2Fe-2S] cluster-bound form of cytosolic monothiol glutaredoxins can be involved in Fe/S protein maturation, via a [2Fe-2S] cluster transfer process from their homodimeric holo states to partner apo proteins, are still lacking.

The human proteome contains only one monothiol glutaredoxin in the cytosol, glutaredoxin-3 (GRX3 hereafter, also commonly named GLRX3 and PICOT). GRX3 consists of three domains: one N-terminal thioredoxin (Trx) domain with no Trx-related enzymatic role[8,17] and two monothiol glutaredoxin (Grx) domains each able to bind a glutathione-coordinated [2Fe-2S] cluster via protein dimerization.[2,18] While the specific function of the *in vivo* indispensable[17] Trx domain is still unknown, the Grx domains of the yeast homologues of GRX3, i.e. Grx3 and Grx4, which can bind one [2Fe-2S] cluster each, are absolutely required for the trafficking of iron in the cytosol and for the regulation of cellular iron homeostasis.[8,14,17] Recently, multiple high-throughput yeast-two-hybrid[19] and affinity capture-MS (BioGRID interaction 1077826) screens show that GRX3 binds *in vivo* anamorsin (also commonly named CIAPIN1), a [2Fe-2S] cluster-binding protein involved in the maturation of cytosolic Fe/S proteins.[20,21] A specific yeast-two-hybrid assay was also performed to identify anamorsin-interacting molecules using mouse anamorsin cDNA as bait and a cDNA library produced from mouse testis.[22] From that study it results that GRX3 is the preferential protein bound to anamorsin in cells. Furthermore, mice either GRX3-deficient ($GRX3^{-/-}$) or anamorsin-deficient ($AM^{-/-}$) are both embryonic lethal. Deletion of the anamorsin gene results in embryonic lethality in late gestation (rate of dead $AM^{-/-}$ embryos 18.8% at embryonic day 14.5) because of a defect in definitive hematopoiesis in the fetal liver,[23,24] while $GRX3^{-/-}$ mice are 100% dead at embryonic day 14.5,[25] although no defects in fetal hematopoiesis are observed in $GRX3^{-/-}$ embryos. Finally, the yeast homologue of anamorsin, Dre2, is found in complexes with Grx3 and Grx4 by a high throughput protein-protein interaction screen,[26] and Fe/S cluster insertion into Dre2 is significantly decreased upon Grx4 depletion, still Dre2 levels being comparable to those detected in in wild-type cells.[8] In conclusion, all together these data provide *in vivo* evidences that GRX3 and anamorsin are physical and functional protein partners involved in the Fe/S cluster assembly process. However, the interaction mode and functional role of this interaction have been not defined yet.

Anamorsin contains two domains: a N-terminal well-folded domain (N-domain, hereafter) of 172 residues, and a largely unstructured C-terminal domain of 90 residues, named Cytokine-Induced Apoptosis INhibitor 1 (CIAPIN1, hereafter), containing two highly conserved cysteine rich motifs able to independently bind a [2Fe-2S] cluster.[20,27] These two domains are connected by a long flexible linker of 50 residues.[27] Anamorsin is an appropriate target to investigate a potential functional role of GRX3 in transferring [2Fe-2S] clusters as: i) it interacts with GRX3;[22] ii) the insertion of the Fe/S cluster into the yeast homologue of anamorsin, Dre2, depends on Grx3 and Grx4, the two cytosolic, functionally redundant yeast homologues of GRX3;[8,14] iii) Fe/S cluster loading on Dre2 is independent of the cytosolic iron-sulfur protein assembly machinery.[21]

In this work the ability of GRX3 in transferring [2Fe-2S] clusters to final target proteins was investigated by studying its interaction with anamorsin. Protein-protein interaction and cluster transfer were studied *in vitro* by a set of spectroscopic techniques. We found that GRX3 transfers two [2Fe-2S] clusters to anamorsin and that the transfer mechanism was dependent on the formation of a specific protein-protein complex between the N-terminal domains of GRX3 and of anamorsin. Their interaction was indeed the fundamental requisite to observe cluster transfer from Grx domains of GRX3 to the CIAPIN1 domain of anamorsin. These findings provide an advanced view of the functional role of GRX3 in iron metabolism.

RESULTS

GRX3 transfers $[2Fe\text{-}2S]^{2+}$ clusters to anamorsin

To investigate Fe/S cluster transfer from GRX3 to anamorsin, a number of GRX3 constructs were prepared: i) full-length GRX3 (fGRX3), ii) a construct lacking the C-terminal Grx domain (GRX3(Trx-GrxA)) that resembles the topological organization of yeast Grx3 and Grx4, iii) a construct containing only the Trx domain (GRX3(Trx)), and iv) a two-domain construct containing both Grx domains (GRX3(GrxA/B)) (**Fig. 1a** and **Supplementary Fig.**

1). All GRX3 constructs were monomeric in their apo form, as determined by analytical gel filtration (**Supplementary Fig. 1** and **Supplementary Results**) and/or by ^{15}N NMR relaxation data, which provided overall reorientational correlation times consistent with monomeric protein states (GRX3(Trx-GrxA) 13.6 ± 1.0 ns, GRX3(Trx) 8.7 ± 0.4 ns, and GRX3(GrxA/B) 12.0 ± 1.2 ns). The Trx domain did not interact with the Grx domains, as indicated by the complete superimposition of the ^{1}H-^{15}N HSQC map of GRX3(Trx) with the signals of the Trx domain in the ^{1}H-^{15}N HSQC maps of apo fGRX3 and apo GRX3(Trx-GrxA) (**Supplementary Fig. 2**). Once chemically reconstituted,fGRX3, GRX3(Trx-GrxA) and GRX3(GrxA/B) dimerized through their Grx domains, each domain bridging a [2Fe-2S] cluster in the oxidized state, as assessed by UV/vis and EPR spectra, analytical gel filtration data and from the Fe/S/protein ratio determination. Specifically, all holo proteins exhibited UV/vis spectra typical of oxidized $[2Fe\text{-}2S]^{2+}$ protein-bound clusters (**Fig. 1b**) and were EPR silent, as expected for the presence of a S=0 ground state of an oxidized $[2Fe\text{-}2S]^{2+}$ cluster. Upon chemical reduction with sodium dithionite, EPR signals of reduced $[2Fe\text{-}2S]^{+}$ protein-bound clusters were observed (**Fig. 1c**). According to gel filtration data and Fe/S/protein ratio quantification performed on the chemically reconstituted samples (**Supplementary Fig. 1** and **Supplementary Table 1**), the species $[2Fe\text{-}2S]_2$-fGRX3$_2$, [2Fe-2S]-GRX3(Trx-GrxA)$_2$ and $[2Fe\text{-}2S]_2$-GRX3(GrxA/B)$_2$ shown in **Fig. 1a** resulted the major species present in solution. These data on fGRX3 and GRX3(GrxA/B) are in agreement with previously reported studies.[2,28] In all dimeric holo GRX3 constructs, the Trx domain did not have intra- and inter-subunit interactions with the Grx domains nor with the Trx domain of the other monomer, as it resulted from the complete superimposition of the ^{1}H-^{15}N HSQC map of GRX3(Trx) with the signals of the Trx domain in the ^{1}H-^{15}N HSQC maps of $[2Fe\text{-}2S]_2$-fGRX3$_2$, and [2Fe-2S]-GRX3(Trx-GrxA)$_2$ (**Supplementary Fig. 2**).

Cluster transfer occurred from either $[2Fe\text{-}2S]_2$-fGRX3$_2$ or [2Fe-2S]-GRX3(Trx-GrxA)$_2$ to apo anamorsin, as followed by UV/vis and EPR spectroscopy. Once the two proteins were

mixed, the absorbance peaks typical of the oxidized $[2Fe\text{-}2S]^{2+}$ cluster of $[2Fe\text{-}2S]_2$-fGRX3$_2$ and [2Fe-2S]-GRX3(Trx-GrxA)$_2$ disappeared and the absorbance peaks typical of the oxidized $[2Fe\text{-}2S]^{2+}$ cluster-bound forms of anamorsin ([2Fe-2S]-anamorsin)[27,29] appeared (**Fig. 1b**). Both anamorsin/GRX3 protein mixtures were EPR silent, in agreement with the presence of the typical S=0 ground state of an oxidized $[2Fe\text{-}2S]^{2+}$ cluster. Upon chemical reduction with sodium dithionite, only EPR signals typical of the reduced $[2Fe\text{-}2S]^{+}$ clusters of [2Fe-2S]-anamorsin were observed (**Fig. 1c**), showing that the clusters were transferred from GRX3 to anamorsin. Incubation of [2Fe-2S]-anamorsin with apo GRX3(Trx-GrxA), even in excess, did not result in any changes of the UV/vis spectrum indicating that the transfer was unidirectional. Finally, UV/vis spectra showed no efficient cluster transfer (less than 10%) when $[2Fe\text{-}2S]_2$-GRX3(GrxA/B)$_2$ was mixed with apo anamorsin (**Fig. 2a**). All these data demonstrated that $[2Fe\text{-}2S]^{2+}$ clusters were transferred from fGRX3 to anamorsin and that the Trx domain of GRX3 was essential to efficiently drive this process.

GRX3/anamorsin interaction promotes cluster transfer

To understand why the Trx domain of GRX3 with no cluster-binding properties drives the observed cluster transfer process, we studied the interaction between the two partner proteins by NMR. As first step, each ^{15}N labelled GRX3 construct in its apo form, i.e. fGRX3, GRX3(Trx-GrxA), GRX3(Trx) and GRX3(GrxA/B), was titrated with unlabeled apo anamorsin. While no effects were observed in the ^{1}H-^{15}N HSQC maps when GRX3(GrxA/B) was mixed with anamorsin (**Fig. 2b**), chemical shift variations and signal broadening effects were observed in the ^{1}H-^{15}N HSQC maps of fGRX3, of GRX3(Trx-GrxA), and of GRX3(Trx) when increasing amounts of anamorsin were added (**Fig. 3a** left panel, and **Supplementary Fig. 3**). In particular, chemical shift changes were limited to the Trx domain signals only, with similar chemical shifts of the Trx domain in the ^{1}H-^{15}N HSQC maps of the three final mixtures (**Fig. 3b** and **Supplementary Fig. 4**). Two not overlapping NH cross-peaks

(assigned to Gln 45 and Ala 47) in the ^{1}H-^{15}N HSQC map of ^{15}N labeled apo GRX3(Trx), whose chemical shifts were largely affected by the protein-protein interaction, were selected to estimate the stoichiometry of the binding. Specifically, upon addition of unlabeled apo anamorsin, the intensity of these two cross-peaks decreased along the unlabeled partner additions, and the formation of two new cross-peaks, assigned to the two corresponding NHs of apo GRX3(Trx) bound to apo anamorsin, was observed with their intensities increasing along the unlabeled partner additions. These two NH resonances of each residue are therefore representative of the free and bound states of GRX3(Trx), respectively. From their intensity ratio in the ^{1}H-^{15}N HSQC maps along the titration, the molar fraction of the two species was determined and plotted against the GRX3(Trx)/anamorsin protein concentration ratio (**Fig. 3a**, right panel). From the analysis of these NMR titration data, it resulted that: i) spectral changes were complete at a 1:1 protein:protein ratio, ii) the NH signals of the Trx domain were affected, while those of the Grx domains in fGRX3 and GRX3(Trx-GrxA) remained essentially unaffected. In the final protein mixtures, line broadening was observed for all backbone NH signals of the ^{15}N labeled protein, even for those with no chemical shift variations, indicating a sizable increase in the molecular weight of the observed species. Therefore, the NMR data indicated the formation of a hetero-complex at a 1:1 ratio between the two proteins in all three protein mixtures, that the Trx domain was essential for the formation of this hetero-complex, and that the Grx domains did not interact with anamorsin in the complex. Gel filtration data performed on the fGRX3/anamorsin protein mixture (**Supplementary Fig. 1**) showed that the hetero-complex is a heterodimer.

To define the interaction site of apo anamorsin with the Trx domain of apo GRX3, the following titrations were performed and followed via ^{1}H-^{15}N HSQC NMR experiments: i) ^{15}N labeled GRX3(Trx) was mixed with the apo CIAPIN1 domain, and then to this mixture unlabeled N-domain of anamorsin was added; ii) ^{15}N labeled apo anamorsin was mixed with unlabeled GRX3(Trx) or fGRX3. In the i) titration, no spectral changes were observed upon

apo CIAPIN1 domain addition, indicating that the CIAPIN1 domain does not interact with the Trx domain of GRX3, while spectral changes were observed upon addition of the N-domain of anamorsin to the GRX3(Trx)/CIAPIN1 domain mixture (**Supplementary Fig. 5**). These data showed that anamorsin recognizes the Trx domain of GRX3 through its N-domain. In agreement with this, in the ii) titration, spectral changes were observed, in the ^{1}H-^{15}N HSQC spectra of apo anamorsin, for the backbone NHs of the N-domain of anamorsin (**Supplementary Fig. 5**).

Overall, the present data showed that apo GRX3 and apo anamorsin form a 1:1 heterodimeric complex through their N-terminal domains and that the CIAPIN1 domain of anamorsin and the Grx domains of GRX3 are not involved in any permanent interaction in this complex. Molecular recognition between the N-terminal domains was therefore the crucial factor determining the complex formation between the two proteins.

Anamorsin linker stabilizes the interaction with GRX3

When ^{15}N labeled GRX3(Trx) was titrated with unlabeled N-domain of anamorsin, nine signals broadened beyond detection in the ^{1}H-^{15}N HSQC spectra and ten signals experienced small chemical shift variation with sizable signal broadening (**Supplementary Fig. 6**). When detecting ^{15}N labeled N-domain of anamorsin, fifteen NH signals broadened beyond detection in the ^{1}H-^{15}N HSQC spectra and twenty two NH signals experienced chemical shift variation with sizable signal broadening (**Supplementary Fig. 6**). A structural model of the complex (**Fig. 4a**), based on these NMR titration data, was calculated with the HADDOCK program.[30] Specifically, the “active” residues (see Methods for the definition of an active residue) engaged in the protein-protein interaction were Gln 45, Ala 47, Gln 48, Glu 51, Val 52, Glu 55, Glu 59, Ala 103, His 104, Ala 105, Glu 107, Thr 109, Lys 110 in GRX3(Trx) and Gln 52, Ala 54, His 55, Glu 57, Glu 78, Arg 85, Ser 117, Leu 121 in the N-domain of anamorsin. The statistics of the final docking calculation was reported in **Supplementary Table 2**. The

residues involved in the protein-protein interaction were located in α-helices 2 and 4 of GRX3(Trx) and in α-helices 2, 3 and 4 and the loop between helix α2 and strand β3 of the N-domain of anamorsin (**Fig. 4a**). This recognition mode between the Trx domain of GRX3 and the N-domain of anamorsin was conserved when the two full-length proteins are made to interact, since the same interacting regions, comprising α-helices 2 and 4 of the Trx domain of GRX3, were identified when ^{15}N labeled apo fGRX3 was titrated with unlabeled apo anamorsin (**Fig. 4a**). However, additional NH signals of the Trx domain of GRX3, located in a negatively charged, Glu-rich, region (Glu 71, Glu 75, Glu 78, and Glu 81) adjacent to the interaction surface, experienced chemical shift changes (**Fig. 4a**). As the CIAPIN1 domain of anamorsin did not interact with the Trx domain of GRX3 (**Supplementary Fig. 5**), these additional observed shifts were necessarily due to the interaction between the unstructured linker region of anamorsin and the Trx domain of GRX3. This additional interacting region is fundamental to stabilize the complex. Indeed, the exchange regime between the free and the bound proteins switched from fast/intermediate, on the NMR time scale, when the N-terminal domains of GRX3(Trx) and of anamorsin interacted, to slow when the N-domain of GRX3(Trx) interacted with full-length anamorsin (**Fig. 4b**), suggesting a significant increase in the protein-protein affinity when the linker is present.[31] According to the structural model of the complex, the C-terminus of the N-domain of anamorsin (where the linker begins) is located near the interaction region (**Fig. 4a**). The first part of the anamorsin linker is rich of positively charged Lys residues (Lys 175, Lys 180, Lys 181, Lys 187), that could electrostatically interact with the Glu-rich region of the Trx domain of GRX3. The presence of this additional protein-protein interaction region was further supported by the disappearance of signals in the unstructured and flexible C-terminal tail of the N-domain of anamorsin (from Phe 166 to Arg 172) in the ^{1}H-^{15}N HSQC NMR spectrum of anamorsin upon complex formation (**Fig. 4a** and **Supplementary Fig. 6**). In conclusion, the NMR/biomolecular docking data here described defined how the N-domains of the two

proteins recognize each other and identified a role of the linker of anamorsin in stabilizing the protein-protein interaction.

Anamorsin complexed with GRX3 binds two $[2Fe\text{-}2S]^{2+}$ clusters

To address whether GRX3/anamorsin complex was still formed once the aforementioned cluster transfer had occurred between $[2Fe\text{-}2S]_2$-fGRX3$_2$ or [2Fe-2S]-GRX3(Trx-GrxA)$_2$ and apo anamorsin, $^{1}H\text{-}^{15}N$ HSQC NMR spectra and analytical gel filtration were performed on ^{15}N labeled $[2Fe\text{-}2S]_2$-fGRX3$_2$/unlabeled apo anamorsin and ^{15}N labeled [2Fe-2S]-GRX3(Trx-GrxA)$_2$/unlabeled apo anamorsin mixtures, at 1:1 protein-protein ratio (considering the monomeric protein concentration for the holo GRX3 constructs). It resulted that i) the $^{1}H\text{-}^{15}N$ HSQC maps of the analyzed constructs of GRX3 in these mixtures were well superimposable with those of the corresponding apo mixtures (**Supplementary Fig. 7**) and ii) gel filtration chromatography showed the presence of a 1:1 heterodimeric complex (**Supplementary Fig. 1**). These data indicated that, in both mixtures, the GRX3 molecule of the 1:1 heterodimeric complex was in the apo state, being thus the [2Fe-2S] cluster(s) bound to anamorsin molecule of the complex, and that the N-terminal domains (Trx of GRX3 and N-domain of anamorsin) interacted in the complex, while the C-terminal, cluster-binding domains (Grxs and CIAPIN1 domains) were not involved in the protein-protein interaction, similarly to what observed in the apo/apo complexes. Additionally, the EPR spectra of the two mixtures (**Fig. 1c**), acquired upon chemical reduction with sodium dithionite, and the paramagnetic IR-^{15}N-HSQC-AP NMR spectra[32], the latter performed on the ^{15}N labeled apo anamorsin/unlabeled [2Fe-2S]-GRX3(Trx-GrxA)$_2$ 1:1 mixture (**Supplementary Fig. 8**), showed EPR parameters and paramagnetic NMR signals typical of the [2Fe-2S]-anamorsin species that binds the clusters through its two conserved cysteine-rich motifs.[29] This indicated that the [2Fe-2S] cluster transfer occurred from both GrxA and GrxB cluster-loaded domains of fGRX3 or from the GrxA cluster-loaded domain of GRX3(Trx-GrxA) to both cluster-

binding sites of the CIAPIN1 domain of anamorsin. Finally, to define whether both metal binding sites of anamorsin in the complex with fGRX3 were fully occupied after the transfer, the Fe:S ratio was quantified before and after $[2Fe\text{-}2S]_2$-$fGRX3_2$ was mixed with apo anamorsin in 1:1 ratio, as described in the Methods section. It resulted that this ratio was unaltered (**Supplementary Table 1**), indicating that anamorsin received two [2Fe-2S] clusters from $[2Fe\text{-}2S]_2$-$fGRX3_2$ and therefore two [2Fe-2S] clusters were bound per protein molecule of ananorsin (**Fig. 5a**). Since we were never able to chemically reconstitute anamorsin with both [2Fe-2S] clusters bound at stoichiometric levels,[20,27,29] the specific protein-protein interaction between fGRX3 and anamorsin was essential to achieve a complete clusters incorporation into anamorsin.

DISCUSSION

We have here shown at the molecular level that GRX3 can play a functional role in cytosolic [2Fe-2S] cluster trafficking, by transferring two [2Fe-2S] clusters to its protein partner anamorsin (**Fig. 5a**). The transfer mechanism was dependent on the formation of a protein-protein complex between the N-terminal domains of GRX3 and of anamorsin. Their interaction was indeed the fundamental requisite to observe [2Fe-2S] cluster transfer from GRX3 to the CIAPIN1 domain of anamorsin (**Fig. 5a**). We suggest that the protein-protein interaction between the N-terminal domains make the cluster binding domains, i.e. the Grx donors and the CAPIN1 acceptor, in the optimal reciprocal orientation for the cluster transfer to occur. Therefore, it appears that the transfer process from GRX3 to anamorsin is a thermodynamically favored process under kinetic control. This mechanism also guarantees that two [2Fe-2S] clusters are concomitantly transferred in a single molecular event to the target protein requiring two [2Fe-2S] clusters.

Once the cluster transfer has occurred, the complex between the two proteins (**Fig. 5a**) then needs to be terminated in the cell, so that the functional process(es) performed by the matured

form of anamorsin can proceed. It has already been shown that holo anamorsin is essential for the cytosolic/nuclear [4Fe-4S] protein assembly and that it is an early step component of the cytosolic iron-sulfur protein assembly (CIA) machinery. Specifically, the matured holo form of anamorsin forms a stable complex with the diflavin reductase NDOR1 in the cell.[20,21] This complex, which receives electrons from NADPH cofactor, has been proposed to act as a source of reducing equivalents for the assembly of target but not scaffold Fe/S cytosolic proteins.[21] It is possible that, once anamorsin has received the clusters from GRX3, the interaction with NDOR1 is favored, thus terminating the interaction with GRX3. Recently, we found that the unstructured linker is the only region of anamorsin that tightly interacts with NDOR1 inducing the formation of a specific and stable protein complex.[20] Indeed, the N-terminal domain of anamorsin was not involved in protein-protein recognition and the C-terminal CIAPIN1 domain of anamorsin, containing the [2Fe-2S] redox center, only transiently interacts, through complementary charged residues, with the FMN-binding domain of NDOR1 to perform the electron transfer reaction.[20] Considering these previous observations and that this study showed that the linker of anamorsin was also involved in the interaction with GRX3, we suggest that, upon interaction of the GRX3-anamorsin complex with NDOR1, the linker might weaken its interaction with GRX3, while favoring the interaction with NDOR1. As the stabilizing effect of the linker on GRX3-anamorsin interaction is then weakened, the binding affinity of the N-terminal domain of GRX3 with that of anamorsin might be decreased, and, as consequence of that, the complex between GRX3 and anamorsin might switch to the complex between anamorsin and NDOR1. The linker interaction is therefore responsible of modulating the formation and release of the various protein-protein complexes responsible to make anamorsin in the redox-competent state able to receive electrons from NDOR1. This multiple functional interactions property of the linker fits well with its high flexibility, which enables its interaction with multiple partners, as commonly observed for intrinsically disordered proteins/regions.[33] This mechanism of action

can also explain how in the cell the interaction between the holo forms of anamorsin and GRX3 is avoided, as the stable interaction between holo anamorsin and NDOR1 will be favored with respect to the interaction of holo anamorsin with holo GRX3.

Our study contributes to the mechanistic understanding of Fe/S protein biogenesis in the cytosol, opening a new molecular view for the cellular function of GRX3 in humans. Our finding, showing that GRX3 plays a key role in maturing anamorsin, indirectly links GRX3 to all anamorsin-dependent cellular processes (**Fig. 5b**). I*n vivo* data showed that silencing of human GRX3 expression in HeLa cells decreases the activities of the cytosolic Fe/S proteins IRP1 and GPAT.[9] This behavior can be a consequence of an impairment of the GRX3-dependent anamorsin maturation process, which makes therefore the CIA machinery unable to function, i.e. to assemble the [4Fe-4S] clusters of IRP1 and GPAT. Similarly, in the functionally homologous yeast system,[8] *in vivo* data showed a decrease of Fe/S cluster insertion into two cytosolic Fe/S protein targets, the [4Fe-4S] proteins Rli1 and Nar1, upon Grx4 depletion, as well as a defect in the di-iron cluster assembling of the cytosolic ribonucleotide reductase, which, similarly to the CIA machinery, depends on the Dre2/anamorsin electron transfer chain.[34,35] In conclusion, by showing that and how GRX3 is able to mature anamorsin, our findings suggest a new molecular interpretation of the available *in vivo* data on GRX3,[8,9,34] thus moving forward the existing functional information on GRX3, i.e. from a limited, intracellular iron trafficking protein towards a new, more complex functional role.

ACKNOLEDGMENTS

We thank Angelo Gallo (CERM) for assistance in recording the EPR spectra. This work was supported by Ente Cassa di Risparmio (Grant ID number: 2013/7101), by the Ministero dell'Istruzione, dell'Università e della Ricerca (Grant ID number: CTN01_00177_962865) and by the European Integrated Structural Biology Infrastructure (INSTRUCT), which is part of the European Strategy Forum on Research Infrastructures, and supported by national member subscriptions.

AUTHOR CONTRIBUTIONS

The work-plan was conceived and designed by L.B. and S.C.-B.; R. M and. K.G. produced protein constructs of anamorsin and GRX3; L.B. and S.C.B. planed the experiments; J.W. and R.P. performed and analyzed NMR data; K.G., J.W. and R.M. performed and analyzed EPR and UV/vis experiments. The manuscript was drafted by L.B. and S.C.-B., and revised by all authors.

COMPETING FINANCIAL INTERESTS STATEMENT

The authors declare no competing financial interests.

REFERENCES

1. Banci, L. *et al.* [2Fe-2S] cluster transfer in iron-sulfur protein biogenesis. *Proc. Natl. Acad. Sci. U. S. A* **111**, 6203-6208 (2014).

2. Haunhorst, P., Berndt, C., Eitner, S., Godoy, J. R. & Lillig, C. H. Characterization of the human monothiol glutaredoxin 3 (PICOT) as iron-sulfur protein. *Biochem. Biophys. Res. Commun.* **394**, 372-376 (2010).

3. Lill, R. *et al.* The role of mitochondria in cellular iron-sulfur protein biogenesis and iron metabolism. *Biochim. Biophys. Acta* **1823**, 1491-1508 (2012).

4. Uzarska, M. A., Dutkiewicz, R., Freibert, S. A., Lill, R. & Muhlenhoff, U. The mitochondrial Hsp70 chaperone Ssq1 facilitates Fe/S cluster transfer from Isu1 to Grx5 by complex formation. *Mol. Biol. Cell* **24**, 1830-1841 (2013).

5. Mapolelo, D. T. *et al.* Monothiol glutaredoxins and A-type proteins: partners in Fe-S cluster trafficking. *Dalton Trans.* **42**, 3107-3115 (2013).

6. Shakamuri, P., Zhang, B. & Johnson, M. K. Monothiol glutaredoxins function in storing and transporting [Fe2S2] clusters assembled on IscU scaffold proteins. *J. Am. Chem. Soc.* **134**, 15213-15216 (2012).

7. Philpott, C. C. Coming into view: eukaryotic iron chaperones and intracellular iron delivery. *J. Biol. Chem.* **287**, 13518-13523 (2012).

8. Muhlenhoff, U. *et al.* Cytosolic monothiol glutaredoxins function in intracellular iron sensing and trafficking via their bound iron-sulfur cluster. *Cell Metab* **12**, 373-385 (2010).

9. Haunhorst, P. *et al.* Crucial function of vertebrate glutaredoxin 3 (PICOT) in iron homeostasis and hemoglobin maturation. *Mol. Biol. Cell* **24**, 1895-1903 (2013).

10. Poor, C. B. *et al.* Molecular mechanism and structure of the Saccharomyces cerevisiae iron regulator Aft2. *Proc. Natl. Acad. Sci. U. S. A* **111**, 4043-4048 (2014).

11. Yamaguchi-Iwai, Y., Stearman, R., Dancis, A. & Klausner, R. D. Iron-regulated DNA binding by the AFT1 protein controls the iron regulon in yeast. *EMBO J.* **15**, 3377-3384 (1996).

12. Rutherford, J. C., Jaron, S., Ray, E., Brown, P. O. & Winge, D. R. A second iron-regulatory system in yeast independent of Aft1p. *Proc. Natl. Acad. Sci. U. S. A* **98**, 14322-14327 (2001).

13. Blaiseau, P. L., Lesuisse, E. & Camadro, J. M. Aft2p, a novel iron-regulated transcription activator that modulates, with Aft1p, intracellular iron use and resistance to oxidative stress in yeast. *J. Biol Chem* **276**, 34221-34226 (2001).

14. Ojeda, L. *et al.* Role of glutaredoxin-3 and glutaredoxin-4 in the iron regulation of the Aft1 transcriptional activator in Saccharomyces cerevisiae. *J. Biol Chem.* **281(26)**, 17661-17669 (2006).

15. Anderson, C. P., Shen, M., Eisenstein, R. S. & Leibold, E. A. Mammalian iron metabolism and its control by iron regulatory proteins. *Biochim. Biophys. Acta* **1823**, 1468-1483 (2012).

16. Li, H. *et al.* The yeast iron regulatory proteins Grx3/4 and Fra2 form heterodimeric complexes containing a [2Fe-2S] cluster with cysteinyl and histidyl ligation. *Biochemistry* **48**, 9569-9581 (2009).

17. Hoffmann, B. *et al.* The multidomain thioredoxin-monothiol glutaredoxins represent a distinct functional group. *Antioxid. Redox. Signal* **15**, 19-30 (2011).

18. Li, H. & Outten, C. E. Monothiol CGFS glutaredoxins and BolA-like proteins: [2Fe-2S] binding partners in iron homeostasis. *Biochemistry* **51**, 4377-4389 (2012).

19. Rual, J. F. *et al.* Towards a proteome-scale map of the human protein-protein interaction network. *Nature* **437**, 1173-1178 (2005).

20. Banci, L. *et al.* Molecular view of an electron transfer process essential for iron-sulfur protein biogenesis. *Proc. Natl. Acad. Sci. U. S. A* **110**, 7136-7141 (2013).

21. Netz, D. J. *et al.* Tah18 transfers electrons to Dre2 in cytosolic iron-sulfur protein biogenesis. *Nat. Chem. Biol.* **6**, 758-765 (2010).

22. Saito, Y. *et al.* PICOT is a molecule which binds to anamorsin. *Biochem. Biophys. Res. Commun.* **408**, 329-333 (2011).

23. Shibayama, H. *et al.* Identification of a cytokine-induced antiapoptotic molecule anamorsin essential for definitive hematopoiesis. *J. Exp. Med.* **199**, 581-592 (2004).

24. Tanimura, A. *et al.* The anti-apoptotic gene Anamorsin is essential for both autonomous and extrinsic regulation of murine fetal liver hematopoiesis. *Exp. Hematol.* **42**, 410-422 (2014).

25. Cha, H. *et al.* PICOT is a critical regulator of cardiac hypertrophy and cardiomyocyte contractility. *J. Mol. Cell Cardiol.* **45**, 796-803 (2008).

26. Tarassov, K. *et al.* An in vivo map of the yeast protein interactome. *Science* **320**, 1465-1470 (2008).

27. Banci, L. *et al.* Anamorsin is a 2Fe2S cluster-containing substrate of the Mia40-dependent mitochondrial protein trapping machinery. *Chem. Biol.* **18**, 794-804 (2011).

28. Li, H., Mapolelo, D. T., Randeniya, S., Johnson, M. K. & Outten, C. E. Human glutaredoxin 3 forms [2Fe-2S]-bridged complexes with human BolA2. *Biochemistry* **51**, 1687-1696 (2012).

29. Banci, L. *et al.* Human anamorsin binds [2Fe-2S] clusters with unique electronic properties. *J. Biol. Inorg. Chem.* **18**, 883-893 (2013).

30. Dominguez, C., Boelens, R. & Bonvin, A. M. HADDOCK: a protein-protein docking approach based on biochemical or biophysical information. *J. Am. Chem. Soc.* **125**, 1731-1737 (2003).

31. Zuiderweg, E. R. Mapping protein-protein interactions in solution by NMR spectroscopy. *Biochemistry* **41**, 1-7 (2002).

32. Ciofi-Baffoni, S., Gallo, A., Muzzioli, R. & Piccioli, M. The IR- 15N-HSQC-AP experiment: a new tool for NMR spectroscopy of paramagnetic molecules. *J. Biomol. NMR* **58**, 123-128 (2014).

33. Oldfield, C. J. & Dunker, A. K. Intrinsically disordered proteins and intrinsically disordered protein regions. *Annu. Rev. Biochem.* **83**, 553-584 (2014).

34. Zhang, Y. *et al.* Conserved electron donor complex Dre2-Tah18 is required for ribonucleotide reductase metallocofactor assembly and DNA synthesis. *Proc. Natl. Acad. Sci. U. S. A* **111**, E1695-E1704 (2014).

35. Zhang, Y. *et al.* Investigation of in vivo diferric tyrosyl radical formation in Saccharomyces cerevisiae Rnr2 protein: requirement of Rnr4 and contribution of Grx3/4 AND Dre2 proteins. *J. Biol. Chem.* **286**, 41499-41509 (2011).

36. Netz, D. J., Pierik, A. J., Stumpfig, M., Muhlenhoff, U. & Lill, R. The Cfd1-Nbp35 complex acts as a scaffold for iron-sulfur protein assembly in the yeast cytosol. *Nat. Chem. Biol.* **3**, 278-286 (2007).

FIGURE LEGENDS

Figure 1: Cluster transfer from GRX3 to anamorsin. (**a**) Schematic representation of GRX3 constructs and anamorsin in their [2Fe-2S] cluster bound forms. (I) and (II) indicate the two cluster-bound species of [2Fe-2S]-anamorsin previously described in Banci *et al.*.[29] Fe and S atoms are represented by red and yellow circles, respectively. (**b**) UV/vis and (**c**) EPR spectra of the isolated proteins and protein mixtures of the cluster transfer experiments. Green lines: $[2Fe\text{-}2S]_2$-$fGRX3_2$; blue lines: [2Fe-2S]-$GRX3(Trx\text{-}GrxA)_2$; red lines: [2Fe-2S]-anamorsin; black lines: 1:1 mixtures of $[2Fe\text{-}2S]_2$-$fGRX3_2$ or of [2Fe-2S]-$GRX3(Trx\text{-}GrxA)_2$ with apo anamorsin. UV/vis spectra of $[2Fe\text{-}2S]_2$-$fGRX3_2$/apo anamorsin mixtures at increasing anamorsin concentrations up to 1:1 protein-protein ratio are reported in dashed line. The EPR g values and UV/vis absorbance maxima typical of the [2Fe-2S] cluster bound forms of anamorsin and GRX3 are reported. In the EPR spectrum of [2Fe-2S]-anamorsin, the g values of the two clusters, each bound to one of the two cysteine-rich motifs of the CIAPIN1 domain of anamorsin, are reported.[29]

Figure 2: Impaired cluster transfer and no protein-protein interaction between GRX3(GrxA/B) and anamorsin. (**a**) Schematic representation of $[2Fe\text{-}2S]_2$-$GRX3(GrxA/B)_2$. UV/vis spectra of $[2Fe\text{-}2S]_2$-$GRX3(GrxA/B)_2$ (orange) and of His-tagged apo anamorsin recorded before (cyano) and after (black) incubation in a ~1:1 protein-protein ratio with $[2Fe\text{-}2S]_2$-$GRX3(GrxA/B)_2$, and its separation through nickel-affinity chromatography, are reported. (**b**) The overlay of ^{1}H-^{15}N HSQC spectra of ^{15}N labeled apo GRX3(GrxA/B) before (black) and after (red) the addition of 1 eq. of apo anamorsin is shown.

Figure 3: apo GRX3 and apo anamorsin specifically recognize each other via their N-terminal domains. (**a**) In the left panel, the overlay of ^{1}H-^{15}N HSQC spectra of ^{15}N labeled

apo GRX3(Trx) before (black) and after (red) the addition of 1 eq. of apo anamorsin is shown. In the right panel, the plot shows the stoichiometric formation of the GRX3-anamorsin complex at the 1:1 protein ratio, as determined by integrating two not overlapping NH cross-peaks of the free (black) and bound (red) state of apo GRX3(Trx) (Gln 45 (●) and Ala 47 (■) marked with rectangles in the ^{1}H-^{15}N HSQC spectra). Data represent mean values ± s.d. ($n \geq 3$). (**b**) Overlay of ^{1}H-^{15}N HSQC spectral regions of ^{15}N labeled apo GRX3(GrxA) (black) and GRX3(Trx) (red) with 1:1 mixtures between ^{15}N labeled apo GRX3(Trx-GrxA) and unlabelled apo anamorsin (green), and between ^{15}N labeled apo GRX3(Trx) and unlabelled apo anamorsin (cyano). Arrows indicate chemical shift changes of NHs belonging to the Trx domain, while NHs of GrxA domain remain essentially unperturbed.

Figure 4: N-domains of apo GRX3 and of apo anamorsin form a heterodimer stabilized through the unstructured linker of anamorsin. (**a**) Backbone NHs (green spheres) experiencing significant spectral changes in the ^{1}H-^{15}N HSQC spectra upon formation of a 1:1 complex between GRX3(Trx) and the N-domain of anamorsin, or between apo fGRX3 and apo anamorsin are mapped on the docking model of GRX3(Trx) (magenta) /N-domain anamorsin (blue) complex. Orange spheres identify residues influenced by the interaction between full-length proteins additional to those (green spheres) observed in the GRX3(Trx)/N-domain complex. Side-chains of the solvent exposed Glu residues on helix α3 of GRX3(Trx) are shown as red sticks, and the first part of the unstructured linker of anamorsin is shown as a dashed blue line with Lys residues indicated as "K circles". (**b**) Overlay of ^{1}H-^{15}N HSQC spectral regions of the ^{15}N labeled N-domain of anamorsin before (black) and after the addition of 0.5 (blue) and 1 (red) eq. of GRX3(Trx) (upper panel) or of apo fGRX3 (lower panel). In the upper panel, arrows illustrate chemical shift deviations of G91 and V125 upon GRX3(Trx) additions, which occur on a fast/intermediate exchange regime on the NMR time scale. In the lower panel, NH chemical shifts of G91 and V125

switch to a slow exchange regime on the NMR time scale upon apo fGRX3 additions. The NH resonances of G91 and V125 showing the presence of free and fGRX3-bound states of the N-domain of anamorsin are shown in black and red, respectively.

Figure 5: Working model for the functional role of cluster transfer from GRX3 to anamorsin in iron metabolism. (**a**) GRX3 dimerized upon binding two [2Fe-2S] clusters through its GrxA and GrxB domains (coral) containing each domain a GSH ligand (green).[28] A specific protein-protein recognition between the N-terminal domains of $[2Fe\text{-}2S]_2$-$fGRX3_2$ and apo anamorsin (in orange and blue, respectively) drives the transfer of the two [2Fe-2S] clusters bound to fGRX3 to the two cysteine-rich motifs of the CIAPIN1 domain of anamorsin. On this basis, a protein-protein adduct, depicted in square bracket, can be assumed as the low populated intermediate required to modulate the cluster transfer process. One molecule of fGRX3 is then released from this intermediate, while the other remains in a complex with anamorsin through the interacting N-terminal domains. The latter complex represents an intermediate product in the cellular environment, as it is expected to be terminated to allow anamorsin performing its electron transfer function in the CIA machinery. (**b**) The here described GRX3-dependent maturation process of holo anamorsin (black box) can affect all cellular processes involving cytosolic and nuclear [4Fe-4S]-dependent proteins, since holo anamorsin, once complexed with NDOR1, is part of a cytosolic electron transfer chain (red arrows) responsible of the maturation of cytosolic/nuclear [4Fe-4S] cluster binding proteins (brown arrows).[21,36] In yeast, Dre2 complexed with Tah18 functions as a source of reducing equivalent to assemble di-iron centers of cytosolic enzymes (light gray arrows).[34] Thus, deficiency in the GRX3-dependent maturation process of anamorsin might affect di-iron cofactor biosynthesis, as observed in yeast.[8]

ONLINE METHODS

Protein production

The cDNA coding for human GRX3 (UniProtKB/Swiss-Prot: O76003) was acquired from Source BioScience. Five different constructs (fGRX3 1–335 aa, GRX3(Trx) 1–117 aa, GRX3(Trx-GrxA) 1–236 aa, GRX3(GrxA/B) 130–335 aa, GRX3(GrxA) 120–236 aa) were amplified by PCR and subsequently inserted into the pETG20A vector using the Gateway technology (Invitrogen). BL21-CodonPlus (DE3)-RIPL Competent *E. coli* cells (Stratagene, La Jolla, CA) were transformed with the obtained plasmids, and cells were grown in LB or minimal media (with $(^{15}NH_4)_2SO_4$ and/or [^{13}C]-glucose) containing 1 mM ampicillin, 1 mM chloramphenicol and 250 μM $FeCl_3$ at 37°C under vigorous shaking until the OD at 600 nm reached 0.6. Protein expression was induced by adding 0.5 mM IPTG and cells were grown over night at 17°C. Cells were harvested by centrifugation at 7500 x g and resuspended in lysis buffer (50 mM Tris-HCl pH 8 containing 500 mM NaCl, 5 mM imidazole, 0.01 mg/ml DNAase, 0.01 mg/ml lysozyme, 1 mM $MgSO_4$, 5 mM GSH and 5 mM DTT). Cell disruption was performed on ice by sonication and the soluble extract, obtained by ultracentrifugation at 40000 x g, was loaded on a HiTrap chelating HP column (GE Healthcare) and the recombinant proteins were eluted with 50 mM Tris-HCl pH 8, 500 mM NaCl and 500 mM imidazole, 5 mM DTT and 5 mM GSH. The proteins were then concentrated with an Amicon Ultra-15 Centrifugal Filter Units with a MWCO of 10 kDa (Millipore). Cleavage of the tag was performed by TEV protease in 50 mM Tris-HCl pH 8, 500 mM NaCl, 5 mM imidazole, 3 mM DTT overnight at room temperature. The protein solution was then loaded on the His Trap column to separate the digested protein from the tag. Size exclusion chromatography was performed as final purification step using a HiLoad Superdex75 16/60 column (GE Healthcare) and degassed 50 mM phosphate buffer pH 7, 5 mM GSH and 5 mM DTT as running buffer. Apo proteins were obtained by addition of 100 mM EDTA and 20 mM $K_4[Fe(CN)_6]$, followed by a gel filtration de-salting column. fGRX3, GRX3(Trx-GrxA),

GRX3(GrxA/B) were chemically reconstituted inside an anaerobic chamber (O_2, < 5 ppm) by incubating the purified proteins in degassed 50 mM Tris, 100 mM NaCl, 5 mM DTT, 5 mM GSH at pH 8 with 1 mM $FeCl_3$ and 1 mM Na_2S over night at room temperature. To prevent the possible interference in the cluster transfer experiments of free [2Fe-2S] clusters, formed in solution in the reconstitution process, a gel filtration de-salting column was performed. Iron and acid-labile sulfide content were determined by colorimetric assays as described in Banci *et al.*.[27]

Human anamorsin (full-length protein, and the N-domain and CIAPIN1 domains) in its apo and [2Fe-2S]-bound form was obtained following previously reported procedures.[20,27,29]

The aggregation state of isolated apo and holo proteins and of protein mixtures was analyzed in air using analytical gel filtration. Purified samples were loaded on a SuperdexTM 75 HR 10/30 analytical column (Amersham Bioscience) pre-equilibrated with 50 mM phosphate buffer pH 7, 5 mM GSH, 5mM DTT and calibrated with the Low Molecular Weight Gel Filtration Calibration kit (GE Healthcare). The buffer was bubbled with N_2 overnight to minimize dissolved O_2 levels. Elution profiles were recorded at 280 nm with a flow rate of 0.5 mL/min.

Protein concentration was determined by Bradford assay[37] using BSA as the calibration standard, and by UV-vis absorbance using extinction coefficient predicted by amno acid protein sequence for the apo protein. The results from each determination were in good agreement.

UV/vis and EPR spectroscopy

UV/vis spectra were anaerobically acquired on a Cary 50 Eclipse spectrophotometer in degassed 50 mM phosphate buffer pH 7, 5 mM GSH and 5 mM DTT. EPR spectra of $[2Fe\text{-}2S]_2$-$fGRX3_2$, [2Fe-2S]-$GRX3(Trx\text{-}GrxA)_2$ and [2Fe-2S]-anamorsin and of the protein mixtures between $[2Fe\text{-}2S]_2$-$fGRX3_2$ or [2Fe-2S]-$GRX3(Trx\text{-}GrxA)_2$ and apo anamorsin were

recorded after the addition, inside an anaerobic chamber, of a degassed sodium dithionite solution to reduce the cluster and the obtained protein solutions were immediately frozen. The EPR spectra were acquired in degassed 50 mM phosphate buffer pH 7, 5 mM GSH, 5 mM DTT and 10% glycerol at 45 K using a Bruker Elexsys E500 spectrometer working at a microwave frequency of ca. 9.45 GHz and equipped with a SHQ cavity and a continuous flow He cryostat (ESR900, Oxford instruments) for temperature control. Acquisition parameters were as following: microwave frequency, 9.640928 GHz; microwave power, 5 mW; modulation frequency, 100 KHz; modulation amplitude, 2.0 G; acquisition time constant, 163.84 ms; number of points 1024; number of scans 8; field range 2300–4300 G or 2800–3800 G.

NMR spectroscopy

Standard ^{1}H-detected triple-resonance NMR experiments for backbone resonance assignment were recorded on 0.5 to 1 mM ^{13}C, ^{15}N labeled samples (apo forms of GRX3(Trx-GrxA), GRX3(Trx) and GRX3(GrxA)) in degassed 50 mM phosphate buffer pH 7, 5 mM DTT at 298 K, using Bruker AVANCE 500 MHz and 700 MHz spectrometers. To identify backbone amide resonances affected by paramagnetic relaxation effects, ^{1}H-^{15}N HSQC edited by a ^{1}H inversion recovery and observed in the antiphase component (IR-^{15}N-HSQC-AP) were collected at 700 MHz and 298 K on apo anamorsin/[2Fe-2S]-GRX3(Trx-GrxA)$_2$ mixture and [2Fe-2S]-anamorsin, prepared in an anaerobic chamber with degassed 50 mM phosphate buffer pH 7, 5 mM GSH, 5 mM DTT.[32] Resonance assignment of apo and [2Fe-2S]-anamorsin was already available.[20,27] All NMR data were processed using the Topspin software package and were analyzed with the program CARA.

Cluster transfer and interaction between GRX3 and anamorsin

To monitor cluster transfer, $[2Fe\text{-}2S]_2$-fGRX3$_2$ and [2Fe-2S]-GRX3(Trx-GrxA)$_2$ was incubated under anaerobic conditions for 30 min with the apo form of anamorsin at increasing anamorsin concentrations up to a 1:1 protein-protein ratio (considering the monomeric protein concentration for the holo GRX3 constructs) in degassed 50 mM phosphate buffer pH 7, 5 mM GSH and 5 mM DTT. Then, UV/vis, EPR and analytical gel filtration were recorded as described above. The same experiment was performed under anaerobic conditions incubating, at a 1:1 protein ratio, [2Fe-2S]-anamorsin and apo fGRX3, and $[2Fe\text{-}2S]_2$-GRX3(GrxA/B)$_2$ and His$_{12}$-tag apo anamorsin.

Protein-protein interaction between ^{15}N labeled apo forms of fGRX3, GRX3(Trx-GrxA), GRX3(GrxA/B), GRX3(Trx) and unlabeled apo anamorsin (full-length, N-domain, CIAPIN1 domain), and ^{15}N labeled apo anamorsin (full-length, N-domain) and unlabeled apo GRX3(Trx) and fGRX3 in degassed 50 mM phosphate buffer pH 7 and 5 mM DTT containing 10% (v/v) D_2O at 298K was investigated by ^{1}H-^{15}N HSQC NMR spectra monitoring spectral changes after addition of increasing amounts of the unlabeled partner. To follow both protein-protein interaction and cluster transfer processes in the same experiment, ^{15}N labeled $[2Fe\text{-}2S]_2$-fGRX3$_2$ or [2Fe-2S]-GRX3(Trx-GrxA)$_2$ was titrated under anaerobic conditions with unlabeled anamorsin, and ^{15}N labeled apo anamorsin with unlabeled [2Fe-2S]-GRX3(Trx-GrxA)$_2$ in degassed 50 mM phosphate buffer pH 7, 5 mM GSH and 5 mM DTT containing 10% (v/v) D_2O at 298K, and the spectral changes were monitored by both ^{1}H-^{15}N HSQC and IR-^{15}N-HSQC-AP NMR spectra.[32]

The structural docking model of the complex between GRX3(Trx) and the N-domain of anamorsin was obtained using HADDOCK program and protocol[38] by the WeNMR portal.[39] In the HADDOCK calculations, the active residues engaged in the protein-protein interaction are those with a high solvent accessibility in the free form of the protein (>50% relative accessibility as calculated with NACCESS) and i) experiencing significant backbone NH chemical shift perturbation upon complex formation (the threshold to define significant

chemical shift perturbations was taken for each protein as the average over all the Δδ values plus 1 σ (standard deviation))[30], or ii) whose NH cross-peaks in ^{1}H-^{15}N HSQC NMR spectra disappeared upon complex formation.

Fe/S cluster quantification

The level of cluster transferred from $[2Fe\text{-}2S]_2$-$fGRX3_2$ to apo anamorsin was quantified performing the following procedure: i) $[2Fe\text{-}2S]_2$-$fGRX3_2$ was titrated under anaerobic conditions with apo anamorsin up to ~ 1 equivalent in degassed 50 mM phosphate buffer pH 7, 5 mM GSH, 5 mM DTT, observing, by UV-vis experiments, the complete transfer of the [2Fe-2S] cluster from fGRX3 to anamorsin; ii) on the starting material $[2Fe\text{-}2S]_2$-$fGRX3_2$ and on the final mixture, the iron and acid-labile sulfur content, and the protein concentration were estimated following the chemical assays described above. The analysis of these data is reported in **Supplementary Table 1**.

METHODS-ONLY REFERENCES

37. Bradford, M. Rapid and Sensitive Method for the Quantitation of Microgram Quantities of Protein Utilizing the Principle of Protein-Dye Binding. *Anal. Biochem.* **72**, 248-254 (1976).

38. de Vries, S. J., van Dijk, M. & Bonvin, A. M. The HADDOCK web server for data-driven biomolecular docking. *Nat. Protoc.* **5**, 883-897 (2010).

39. Wassenaar, T. A. *et al.* WeNMR: Structural Biology on the Grid. *Journal of Grid Computing* **10**, 743-767 (2012).

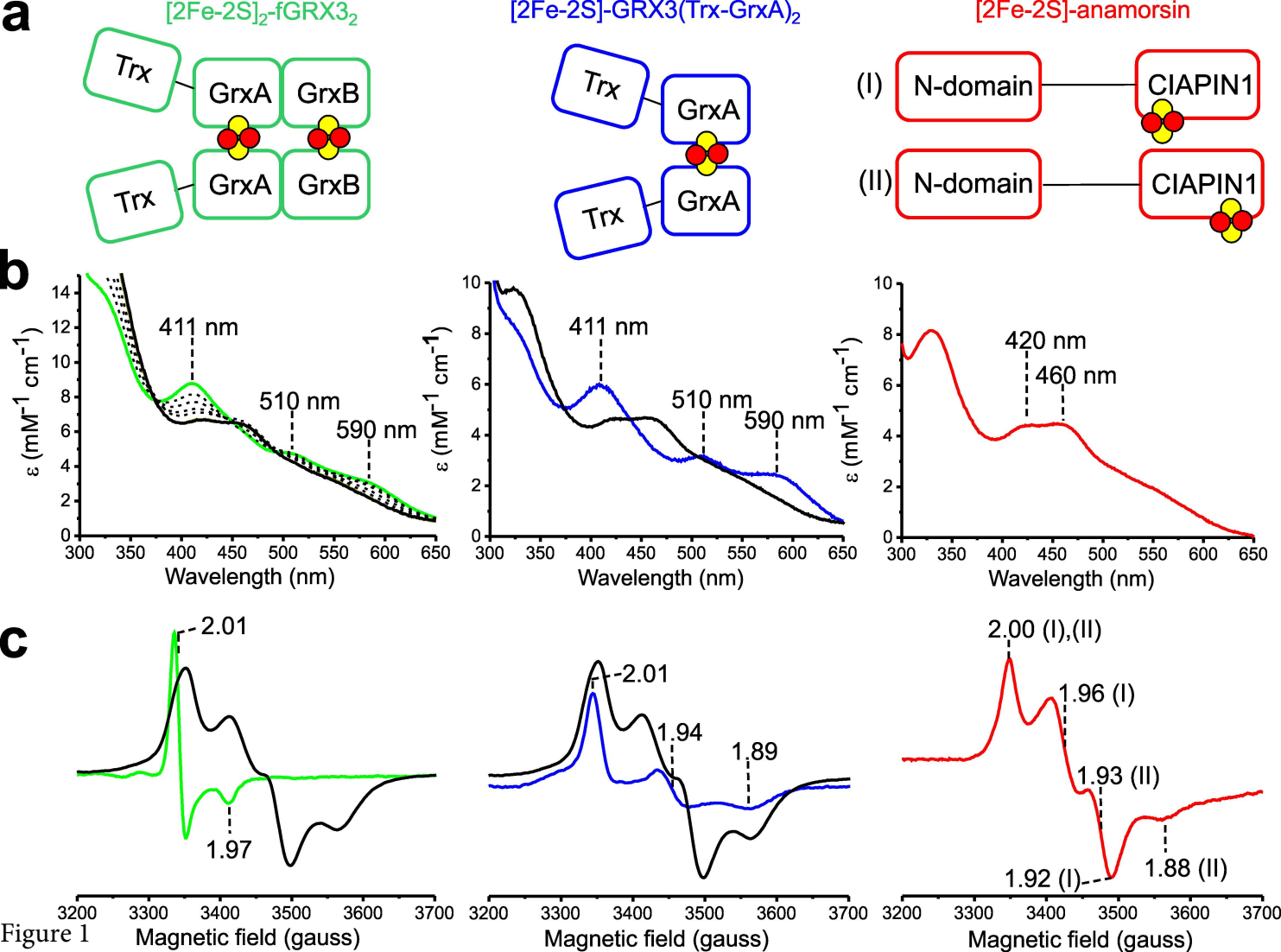
a
[2Fe-2S]2-fGRX32
Trx
GrxA
GrxB
Trx
GrxA
GrxB
[2Fe-2S]-GRX3(Trx-GrxA)2
Trx
GrxA
Trx
GrxA
[2Fe-2S]-anamorsin
(I) N-domain
CIAPIN1
(II) N-domain
CIAPIN1
b
411 nm
510 nm
590 nm
ε (mM-1 cm-1)
Wavelength (nm)
411 nm
510 nm
590 nm
ε (mM-1 cm-1)
Wavelength (nm)
420 nm
460 nm
ε (mM-1 cm-1)
Wavelength (nm)
c
2.01
1.97
Magnetic field (gauss)
2.01
1.94
1.89
Magnetic field (gauss)
2.00 (I),(II)
1.96 (I)
1.93 (II)
1.92 (I)
1.88 (II)
Magnetic field (gauss)

Figure 1

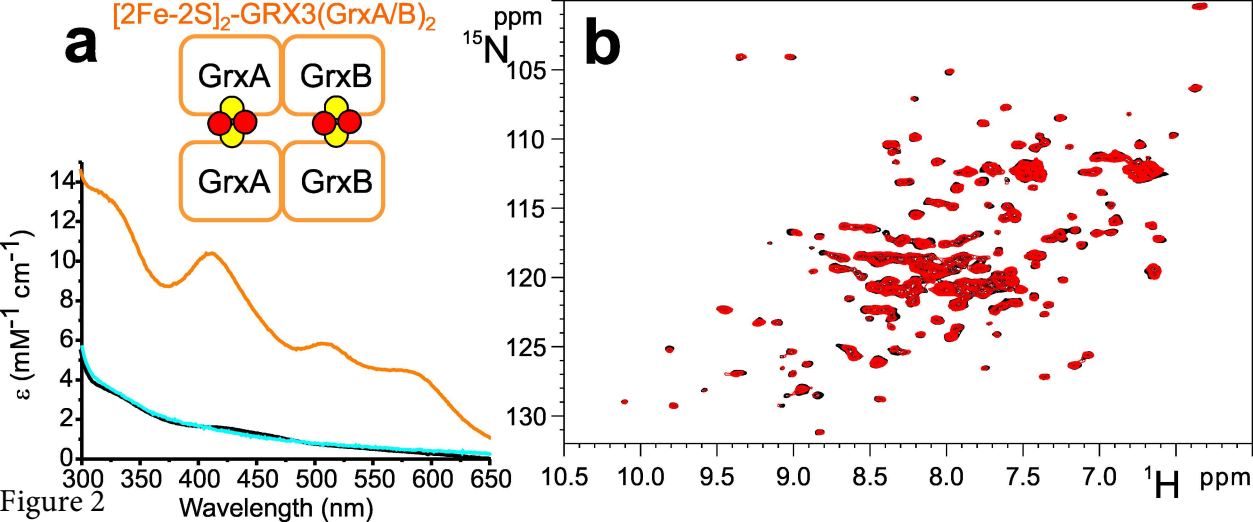
a
[2Fe-2S]2-GRX3(GrxA/B)2
GrxA
GrxB
GrxA
GrxB
ε (mM-1 cm-1)
Wavelength (nm)
b
ppm
15N
1H ppm

Figure 2

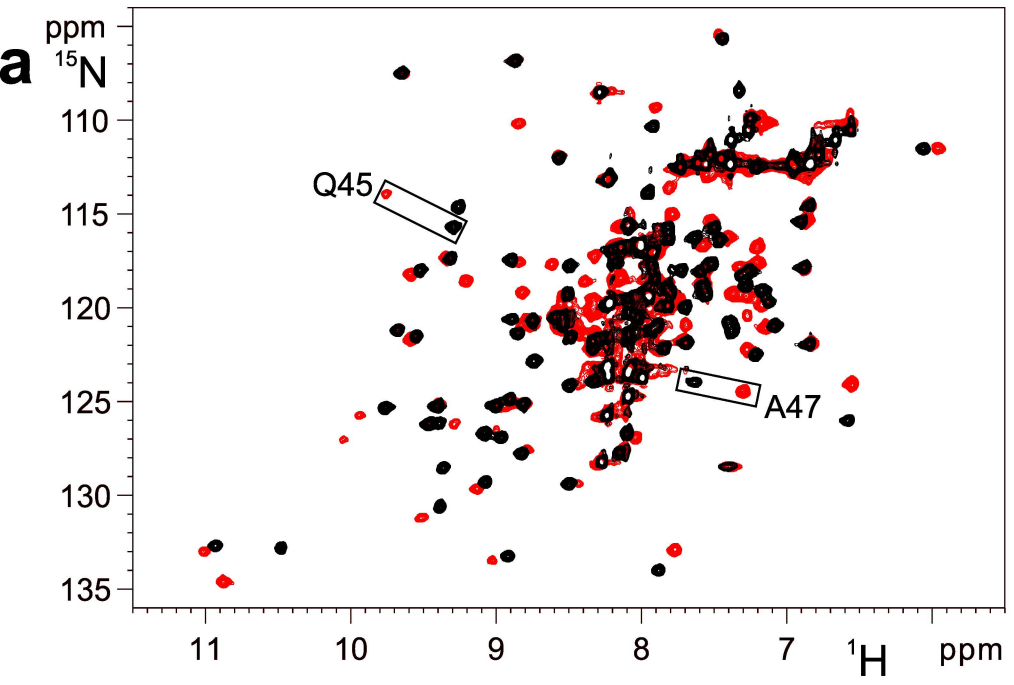
a
ppm
15N
110
115
120
125
130
135
Q45
A47
11
10
9
8
7
1H
ppm

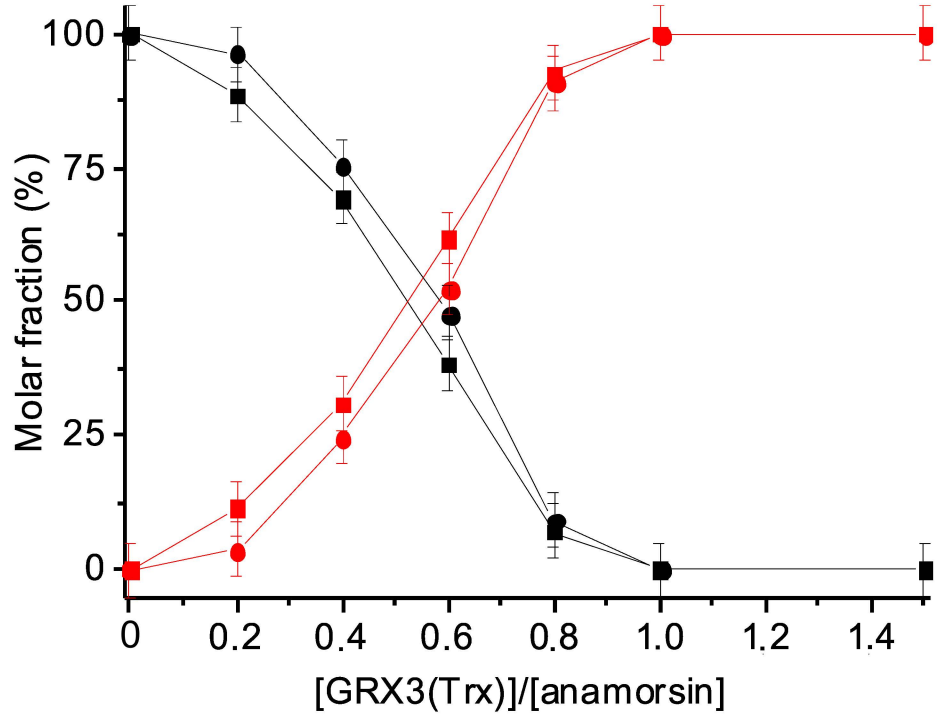
100
75
50
25
0
Molar fraction (%)
0
0.2
0.4
0.6
0.8
1.0
1.2
1.4
[GRX3(Trx)]/[anamorsin]

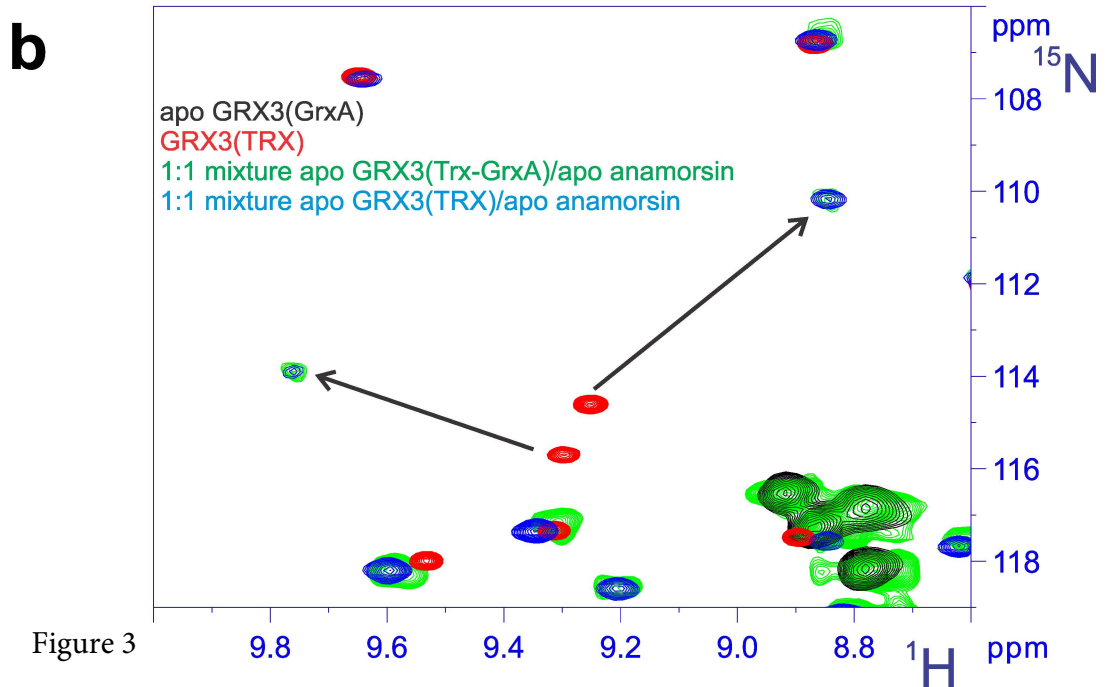
b
apo GRX3(GrxA)
GRX3(TRX)
1:1 mixture apo GRX3(Trx-GrxA)/apo anamorsin
1:1 mixture apo GRX3(TRX)/apo anamorsin
ppm
15N
108
110
112
114
116
118
9.8
9.6
9.4
9.2
9.0
8.8
1H
ppm

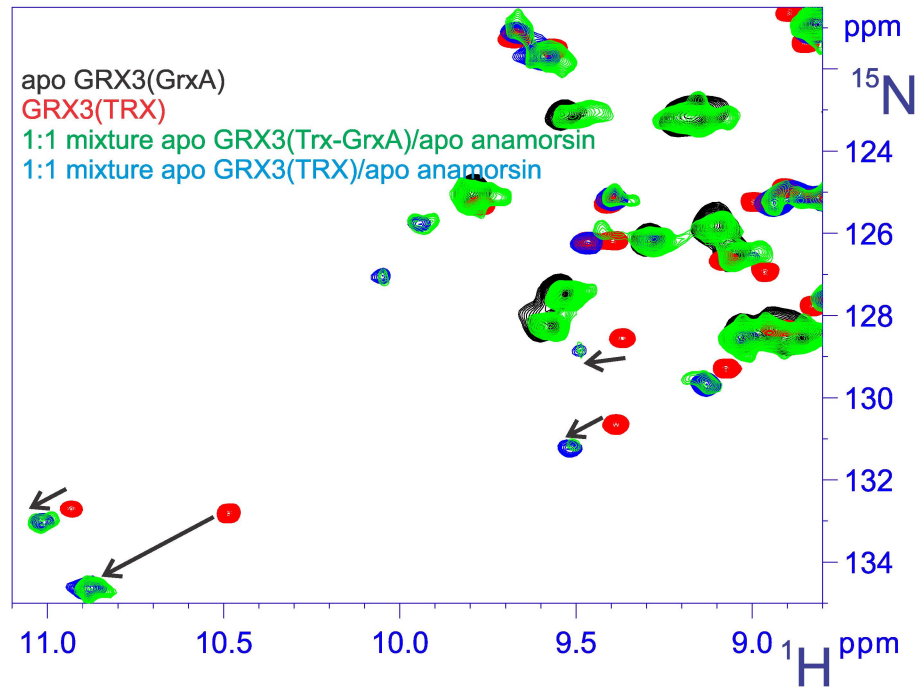
apo GRX3(GrxA)
GRX3(TRX)
1:1 mixture apo GRX3(Trx-GrxA)/apo anamorsin
1:1 mixture apo GRX3(TRX)/apo anamorsin
ppm
15N
124
126
128
130
132
134
11.0
10.5
10.0
9.5
9.0
1H
ppm

Figure 3

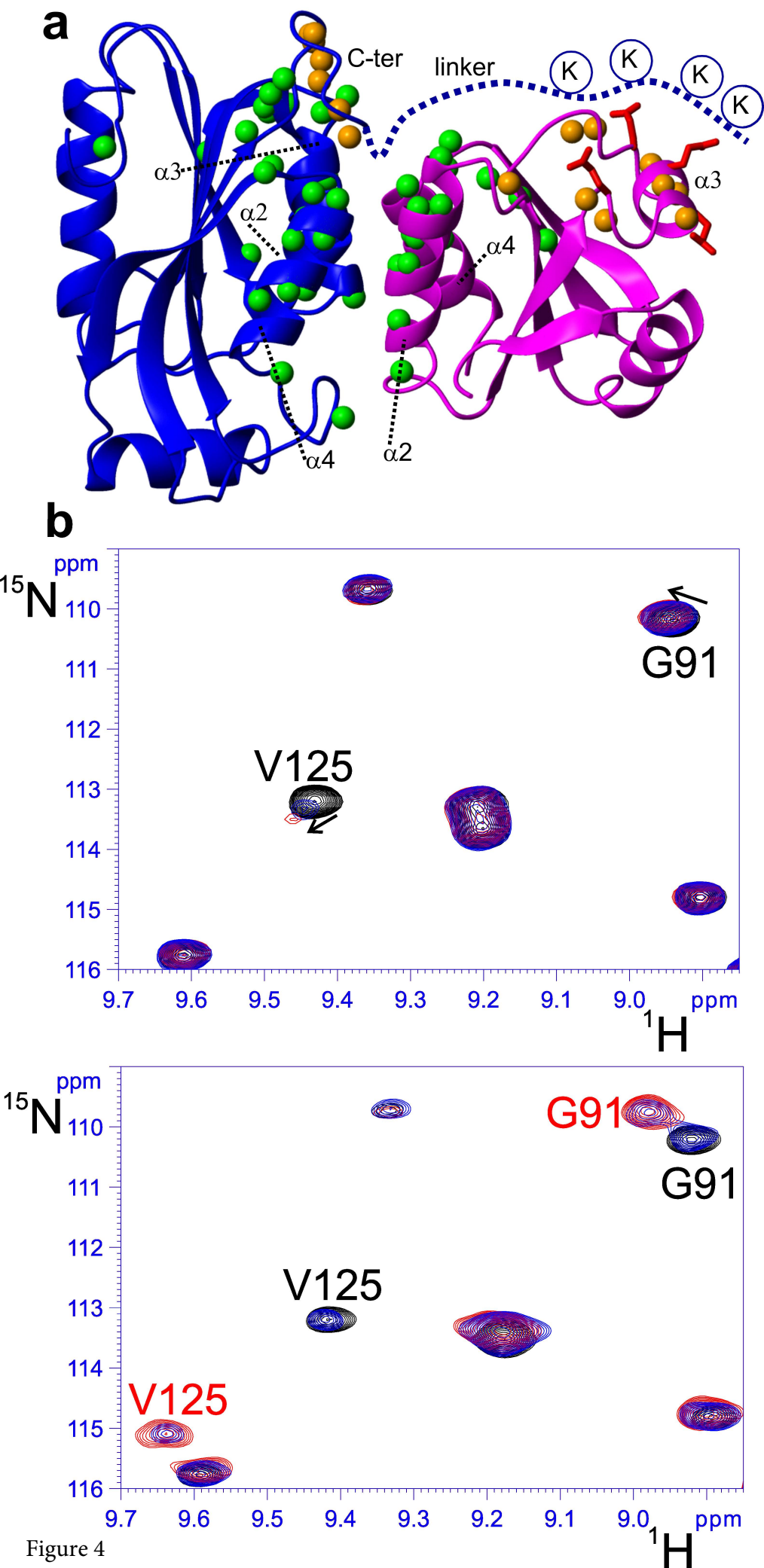
a
C-ter
linker
K
K
K
K
α3
α2
α4
α3
α4
α2
b
ppm
15N
110
111
112
113
114
115
116
G91
V125
9.7
9.6
9.5
9.4
9.3
9.2
9.1
9.0
ppm
1H
ppm
15N
110
111
112
113
114
115
116
G91
G91
V125
V125
9.7
9.6
9.5
9.4
9.3
9.2
9.1
9.0
ppm
1H

Figure 4

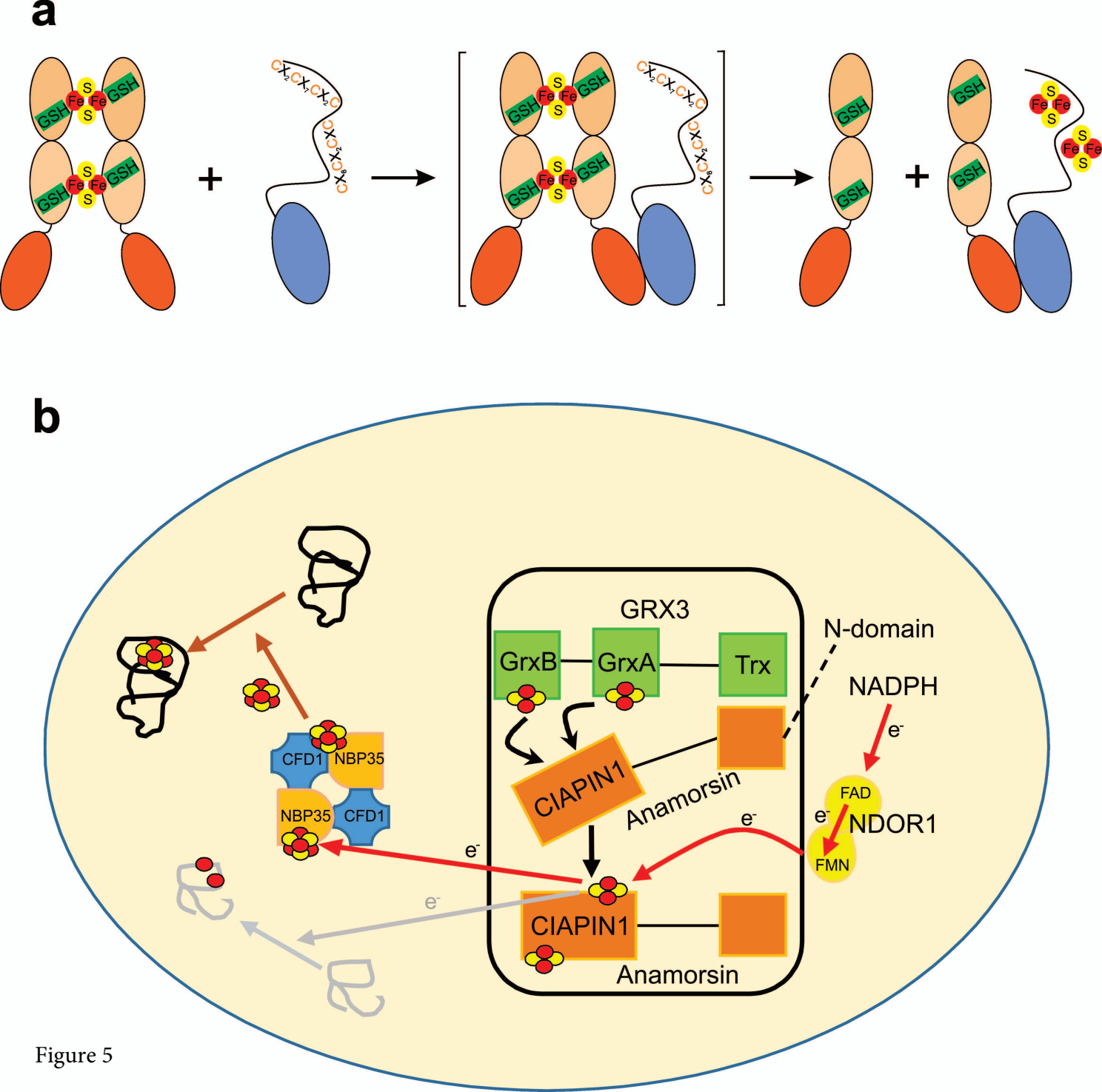
a
GSH
Fe
S
b
GRX3
GrxB
GrxA
Trx
N-domain
NADPH
e-
CIAPIN1
Anamorsin
FAD
NDOR1
FMN
CFD1
NBP35

Figure 5

Supplementary Information

N-terminal domains mediate [2Fe-2S] cluster transfer from glutaredoxin-3 to anamorsin

Lucia Banci[1,2,*], Simone Ciofi-Baffoni[1,2,*], Karolina Gajda[1], Riccardo Muzzioli[1,2], Riccardo Peruzzini[1], Julia Winkelmann[1]

[1]Magnetic Resonance Center CERM, University of Florence, Via Luigi Sacconi 6, 50019, Sesto Fiorentino, Florence, Italy

[2]Department of Chemistry, University of Florence, Via della Lastruccia 3, 50019 Sesto Fiorentino, Florence, Italy

Supplementary Results

Supplementary Table 1. Iron, and acid-labile sulfide analyses of fGRX3, GRX3(Trx-GrxA), GRX3(GrxA/B), anamorsin and of fGRX3/anamorsin 1:1 hetero-complex.

Sample	Fe[a]	S[a]
Chemically reconstituted [2Fe-2S] fGRX3	4.2 ± 0.1	4.1 ± 0.1
Chemically reconstituted [2Fe-2S] GRX3(Trx-GrxA)	1.8 ± 0.1	1.9 ± 0.1
Chemically reconstituted [2Fe-2S] GRX3(GrxA/B)	4.0 ± 0.1	4.1 ± 0.1
[2Fe-2S] anamorsin	2.1 ± 0.1	2.0 ± 0.1
[2Fe-2S] fGRX3 - apo anamorsin 1:1 complex	3.9 ± 0.1	4.3 ± 0.1

[a]Fe and acid-labile S measurements are reported as mol Fe or S per mol of complex (homodimer or heterodimer) and of anamorsin. Fe and S measurements are obtained from two independent samples. Data represent mean values ± s.d.

Supplementary Table 2. Parameters of the data-driven docking model of the complex between GRX3(Trx) and the N-domain of anamorsin. Data represent mean values ± s.d. obtained from 200 structures clustered in 1 cluster.

HADDOCK score	-75.1 ± 1.5
Cluster size	200
RMSD from the overall lowest-energy structure	0.5 ± 0.3
Van der Waals energy	-33.5 ± 1.7
Electrostatic energy	-430.9 ± 39.3
Desolvation energy	39.6 ± 6.2
Restraints violation energy	51.0 ± 3.6
Buried Surface Area	1454.0 ± 24.2
Z-Score	0.0

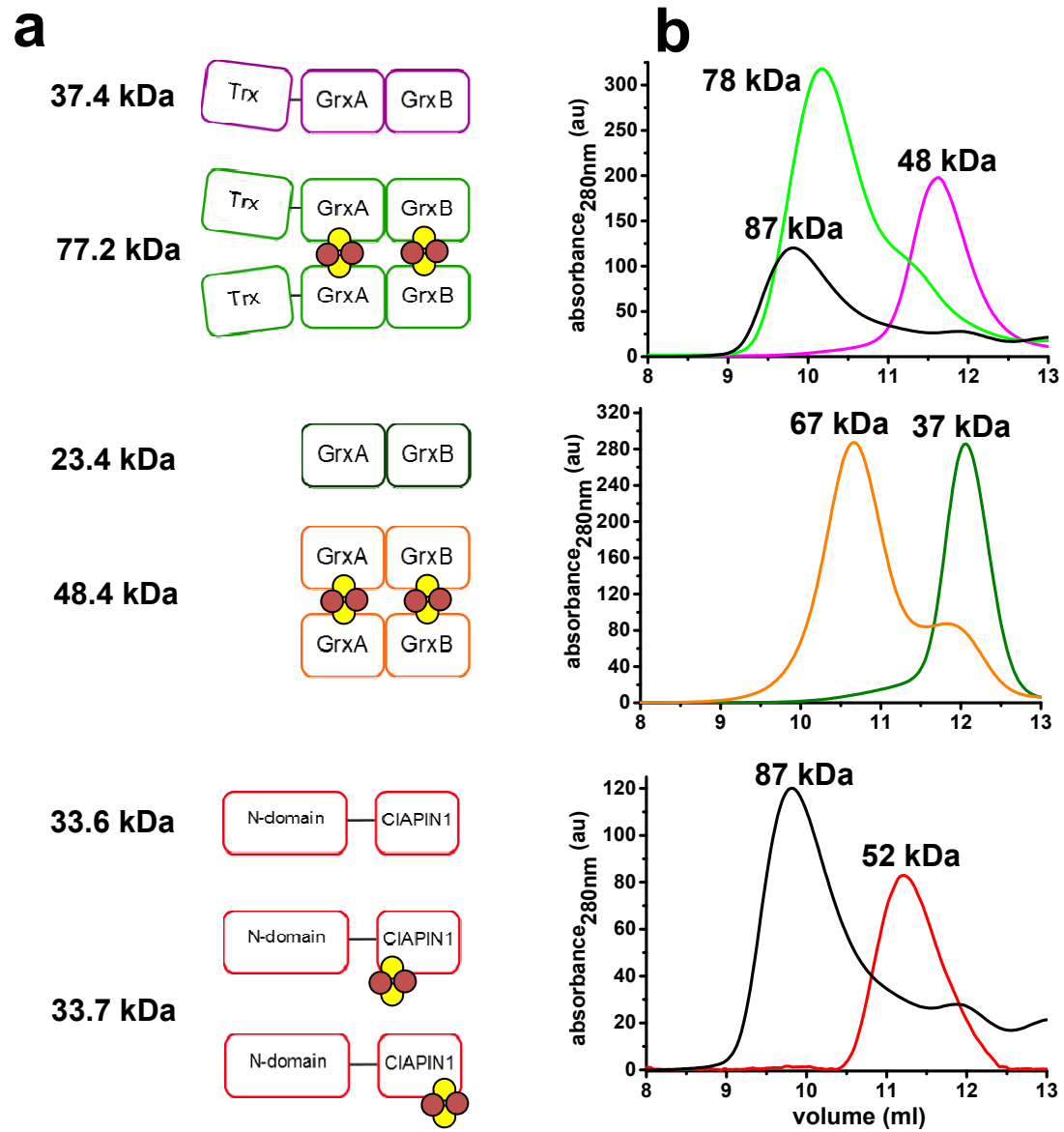

Supplementary Fig. 1. Spectoscopic and aggregation properties of apo/holo forms of GRX3 and anamorsin before and after their interaction. (**a**) Schematic representation of fGRX3, GRX3(GrxA/B) and anamorsin in their apo and [2Fe-2S] cluster bound forms with their corresponding theoretical masses reported on the left. Fe and S atoms are represented by red and yellow circles, respectively. (**b**) Analytical gel filtration chromatograms of isolated proteins in their apo and holo states and of the protein mixtures analyzed in this study. Purple line: apo fGRX3; green line: $[2Fe\text{-}2S]_2$-$fGRX3_2$; dark green line: apo GRX3(GrxA/B); orange line: $[2Fe\text{-}2S]_2$-$GRX3(GrxA/B)_2$; red line: apo or [2Fe-2S]-anamorsin; black line: 1:1 mixture of apo or $[2Fe\text{-}2S]_2$-$fGRX3_2$ with apo anamorsin. The experimental masses reported at the top of each chromatographic peak derive from analytical gel filtration analysis.

Supplementary Fig. 2. Monitoring by NMR the intra- and inter-subunit interactions of the Trx domain of fGRX3 with the Trx and Grx domains. (**a**) Overlay of ^{1}H-^{15}N HSQC spectra of ^{15}N labeled GRX3(Trx) (red) and of ^{15}N labeled apo fGRX3 (black) recored at 900MHz. (**b**) Overlay of ^{1}H-^{15}N HSQC spectra of ^{15}N labeled GRX3(Trx) (red) and of ^{15}N labeled apo GRX3(Trx-GrxA) (black) recored at 900MHz. (**c**) Overlay of ^{1}H-^{15}N HSQC spectra of ^{15}N labeled GRX3(Trx) (red) and of ^{15}N labeled $[2Fe\text{-}2S]_2$-$fGRX3_2$ (black) recored at 900MHz. (**d**) Overlay of ^{1}H-^{15}N HSQC spectra of ^{15}N labeled GRX3(Trx) (red) and of ^{15}N labeled [2Fe-2S]-$GRX3(Trx\text{-}GrxA)_2$ (black) recored at 900MHz.

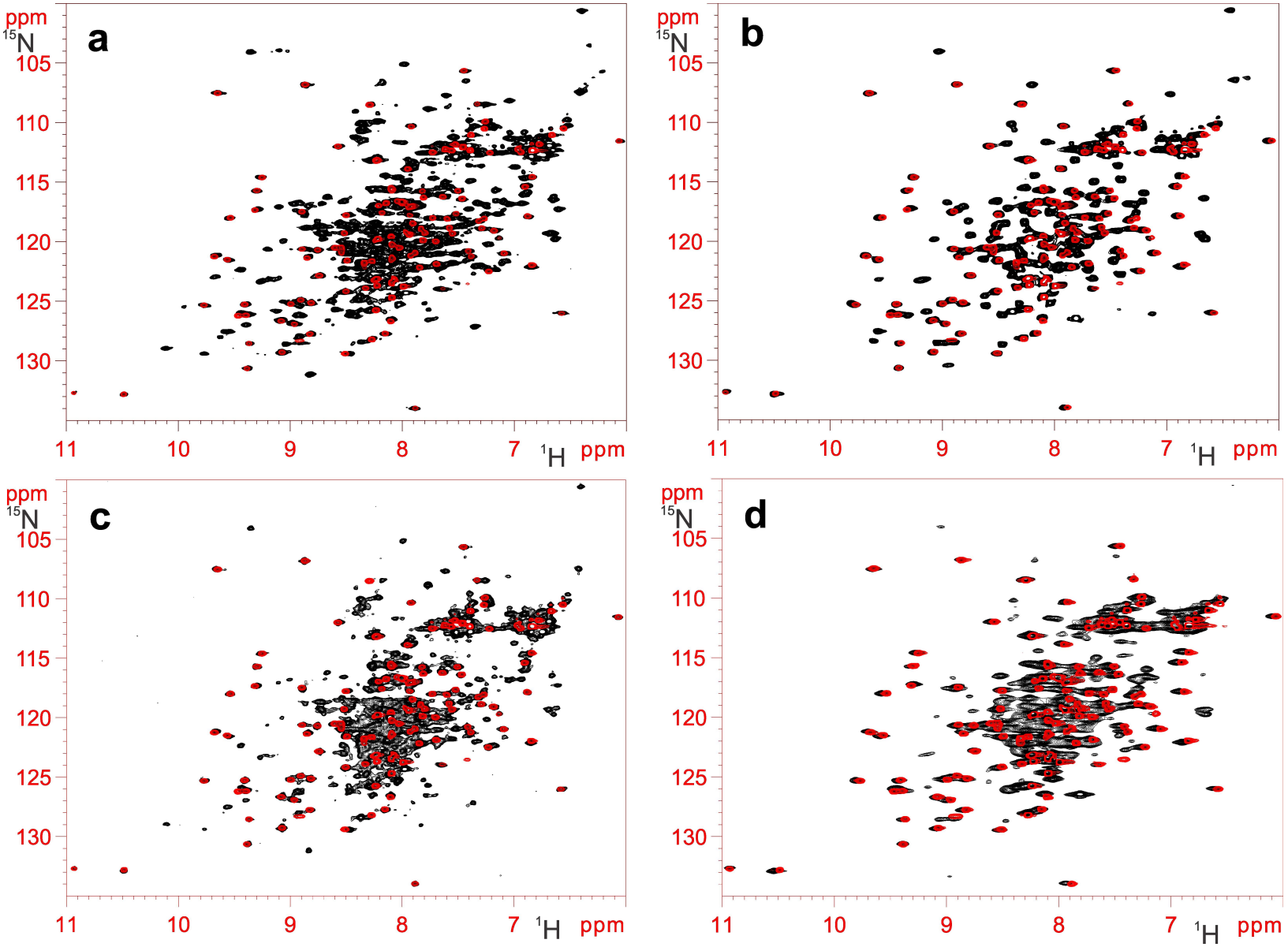

Supplementary Fig. 3. Monitoring by NMR the interaction between different constructs of GRX3 and full-length anamorsin in their apo forms. (**a**) Overlay of ^{1}H-^{15}N HSQC spectra of ^{15}N labeled apo GRX3(Trx-GrxA) (black) and of a 1:1 mixture between ^{15}N labeled apo GRX3(Trx-GrxA) and unlabelled apo anamorsin (red). (**b**) Overlay of ^{1}H-^{15}N HSQC spectra of ^{15}N labeled apo fGRX3 (black) and of a 1:1 mixture between ^{15}N labeled apo fGRX3 and unlabelled apo anamorsin (red). (**c**) Overlay of ^{1}H-^{15}N HSQC spectra of the two mixtures, i.e. 1:1 mixture between ^{15}N labeled apo GRX3(Trx-GrxA) and unlabelled apo anamorsin (black) and 1:1 mixture between ^{15}N labeled apo fGRX3 and unlabelled apo anamorsin (red).

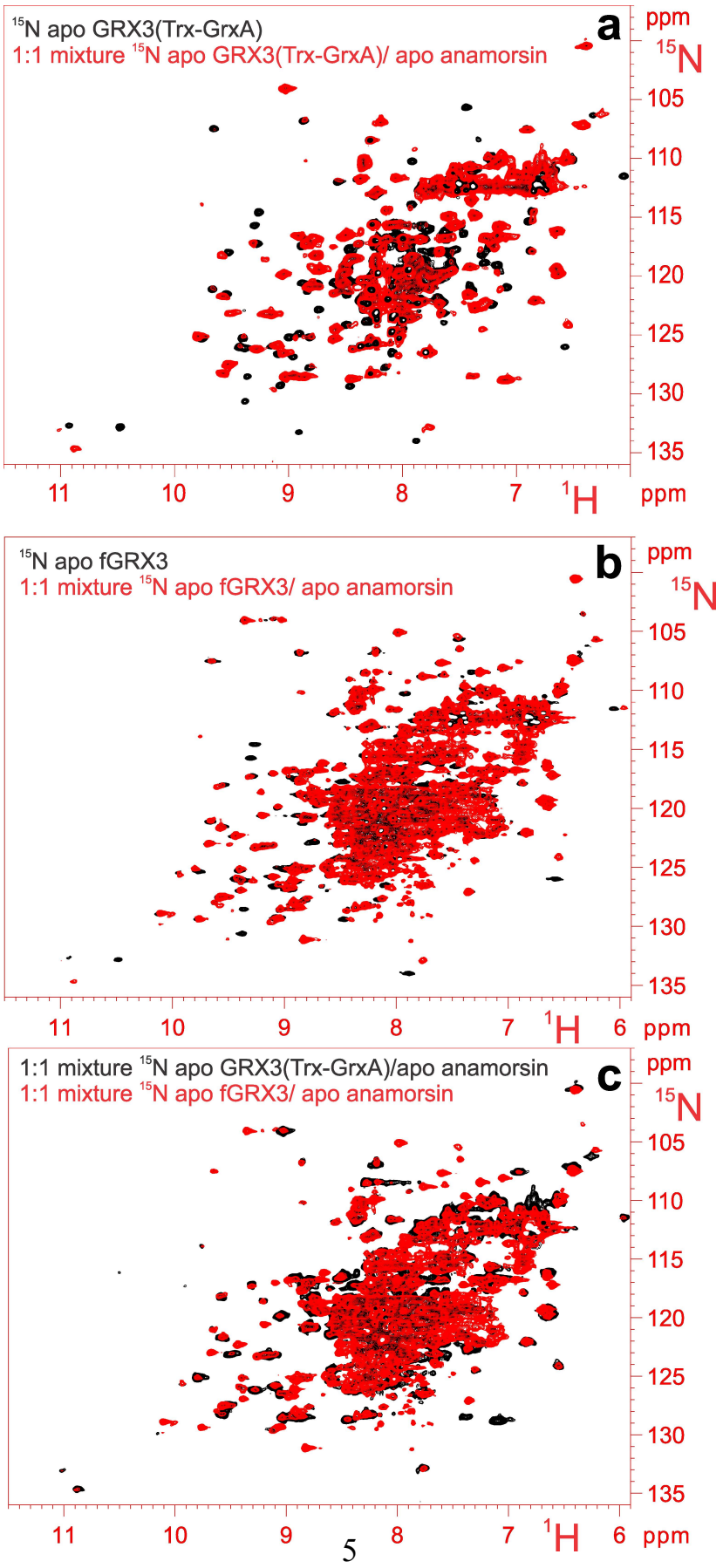

Supplementary Figure 4: NMR analysis of the interaction between different constructs of GRX3 and full-length anamorsin in their apo forms Overlay of ^{1}H-^{15}N HSQC spectral regions of ^{15}N labeled apo GRX3(GrxA/B) (black) and GRX3(TRX) (red) GRX3 with 1:1 mixtures between ^{15}N labeled apo GRX3(Trx-GrxA) and unlabelled apo anamorsin (green), and between ^{15}N labeled apo fGRX3 and unlabelled apo anamorsin (cyano). Arrows indicate chemical shift changes of NHs belonging to the Trx domain, while NHs of GrxA and GrxB domains remain essentially unperturbed.

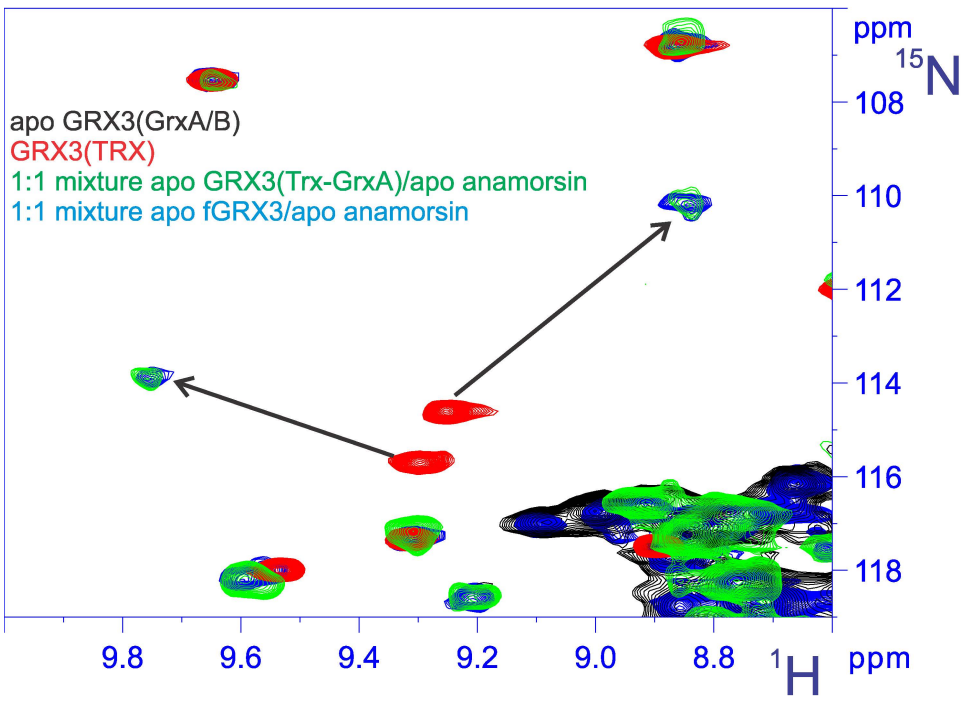

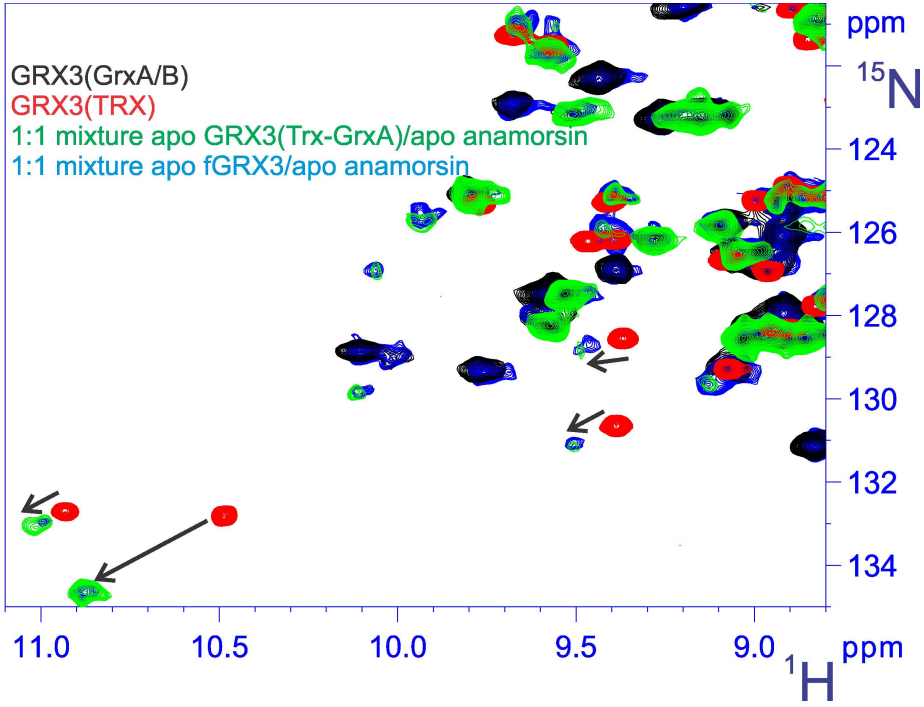

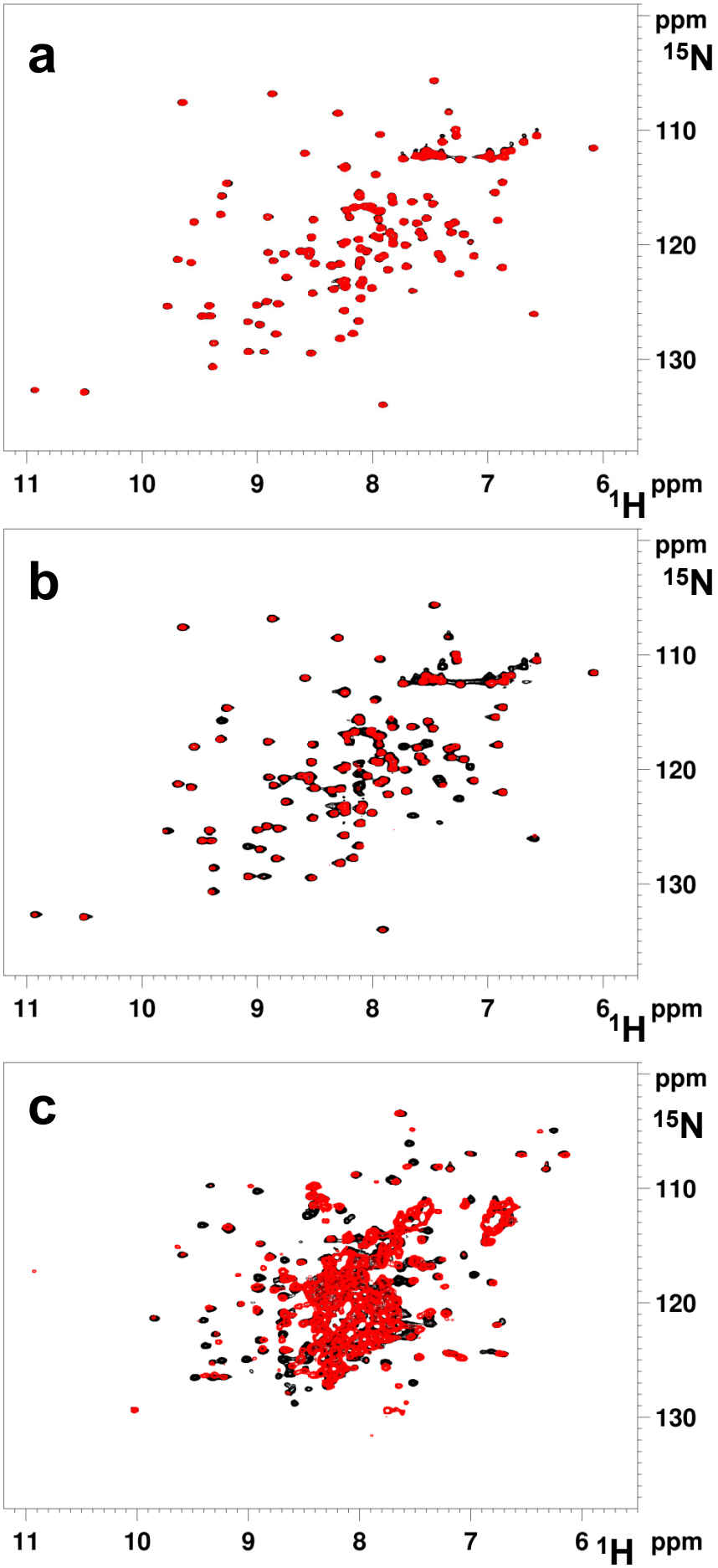

Supplementary Fig. 5. Monitoring by NMR the interaction site of apo anamorsin with the Trx domain of apo GRX3. (**a**) Overlay of ^{1}H-^{15}N HSQC spectra, recorded at 700 MHz and 298 K, of ^{15}N labeled GRX3(Trx) before (black) and after (red) incubation with 1 eq. of the apo form of the CIAPIN1 domain of anamorsin, and (**b**) before and after addition of 1 eq. of the N-domain of anamorsin to this mixture. (**c**) Overlay of ^{1}H-^{15}N HSQC spectra of ^{15}N labeled apo anamorsin before (black) and after (red) incubation with 1 eq. of GRX3(Trx) recorded at 800 MHz and 298 K.

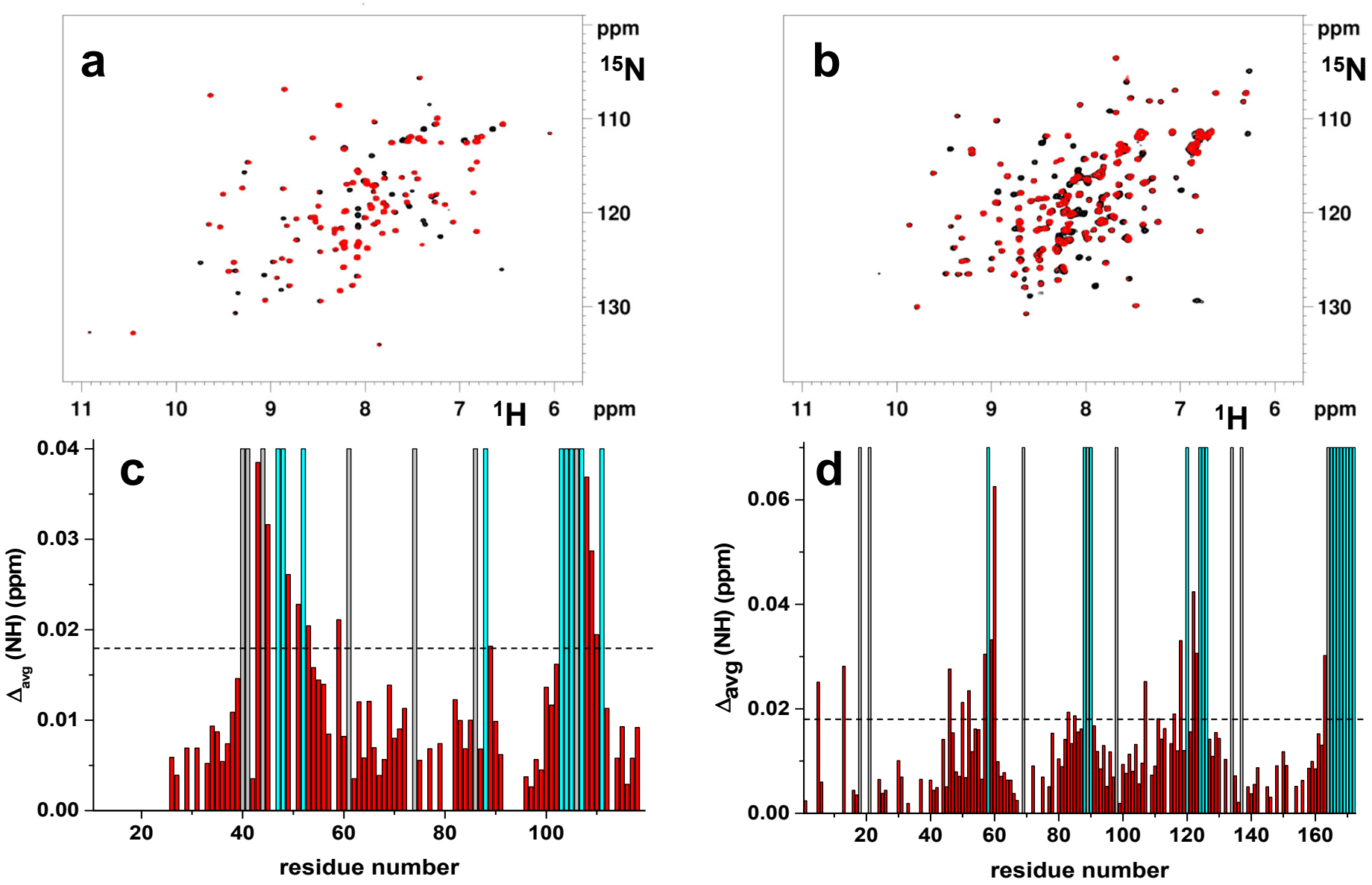

Supplementary Fig. 6. NMR analysis of the protein-protein interaction between the N-terminal domains of GRX3 and anamorsin. Overlay of ^{1}H-^{15}N HSQC spectra of ^{15}N labeled GRX3(Trx) (**a**) and of ^{15}N labeled N-domain of anamorsin (**b**) before (black) and after (red) incubation with 1 eq. of the N-domain of anamorsin and GRX3(Trx), respectively, recorded at 950MHz and 800MHz, respectively. Backbone weighted average chemical shift differences Δ_{avg}(HN) (i.e. $((\Delta H)^2 + (\Delta N/5)^2)/2)^{1/2}$, where ΔH and ΔN are chemical shift differences for ^{1}H and ^{15}N, respectively) versus residue numbers, observed upon addition of 1 eq. of the unlabelled N-domain of anamorsin to ^{15}N-labeled GRX3(Trx) (**c**), and upon addition of 1 eq. of unlabelled GRX3(Trx) to ^{15}N labeled N-domain of anamorsin (**d**). Gray bars indicate Pro residues and the unassigned backbone NH of Ala 40 of GRX3(Trx), cyano bars indicate backbone NHs which broadened beyond detection. Thresholds of 0.018 ppm (mean value of Δ_{avg}(HN) plus 1σ, black dashed line) were used in both titrations to identify significant chemical shift differences.

Supplementary Fig. 7. Monitoring by NMR the interaction between [2Fe-2S] cluster-bound forms of GRX3 and apo anamorsin. (**a**) Overlay of ^{1}H-^{15}N HSQC spectra of a 1:1 mixture of ^{15}N labeled [2Fe-2S]-GRX3(Trx-GrxA)$_2$/unlabeled apo anamorsin (red) and a 1:1 mixture of ^{15}N labeled apo GRX3(Trx-GrxA)/unlabeled apo anamorsin (black). (**b**) Overlay of ^{1}H-^{15}N HSQC spectra of a 1:1 mixture of ^{15}N labeled [2Fe-2S]$_2$-fGRX3$_2$/unlabeled apo anamorsin (red) and a 1:1 mixture of ^{15}N labeled apo fGRX3/unlabeled apo anamorsin (black).

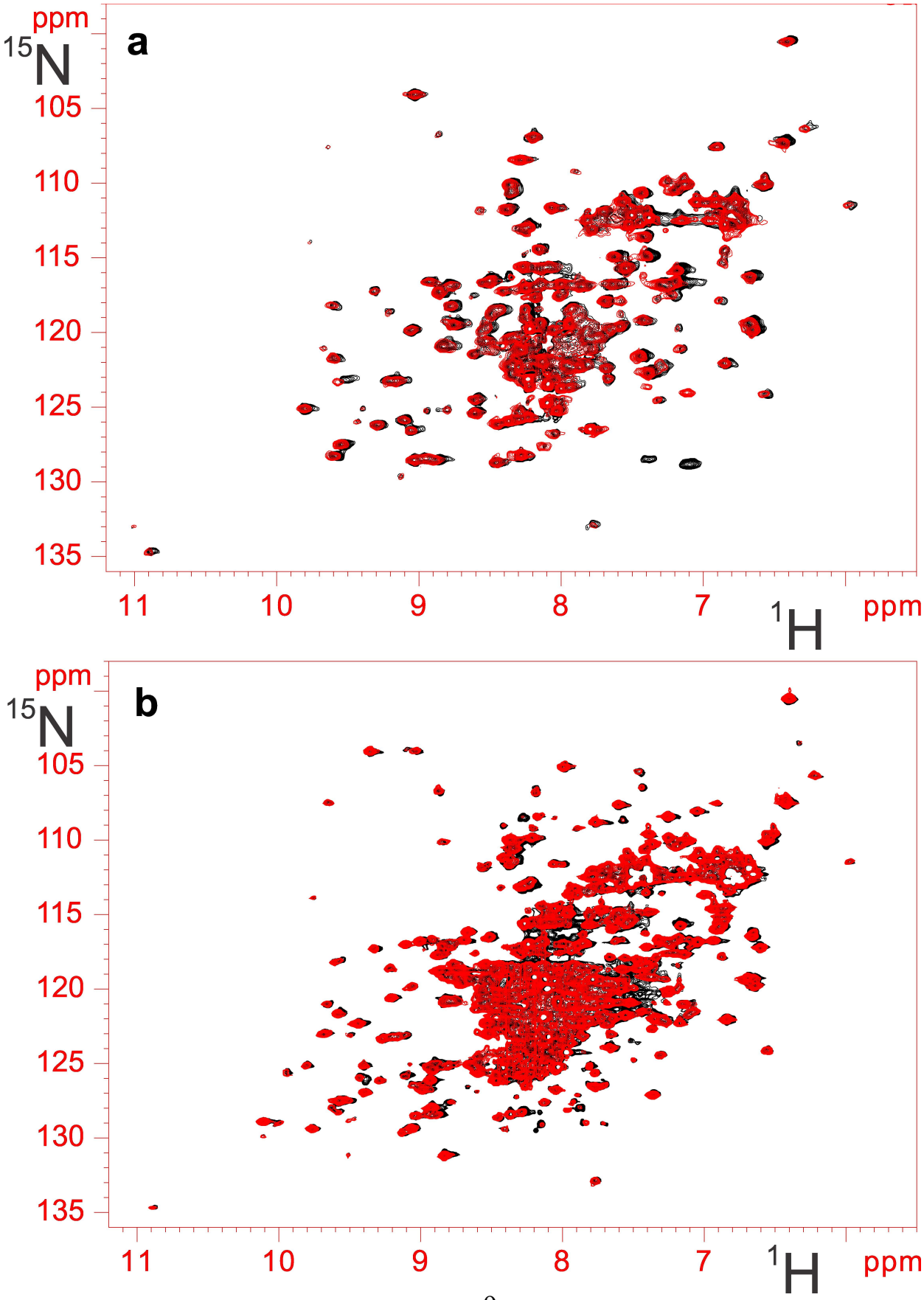

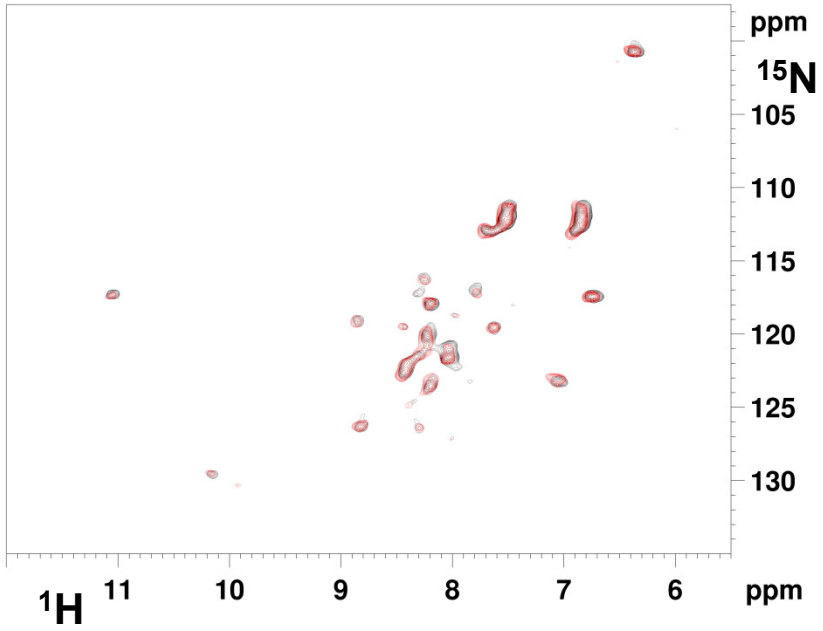

Supplementary Fig. 8. Paramagnetic NMR spectra to monitor cluster transfer from [2Fe-2S]-GRX3(Trx-GrxA)$_2$ to apo anamorsin. Overlay of paramagnetic IR-^{15}N-HSQC-AP spectra of a ~1:1 apo anamorsin/[2Fe-2S]-GRX3(Trx-GrxA)$_2$ mixture (black) and of [2Fe-2S]- anamorsin (red) recorded at 700MHz and 311K.